Biodegradable Metals as Temporary Implants: historically from Beside to Bench and back.

F Witte[1]

[1] *Laboratory for Biomechanics and Biomaterials, Orthopaedic Clinic, Hannover Medical School, Germany.* [2]

INTRODUCTION: The concept of temporary implants made of metals which corrode *in vivo* is creating irritation since it contradicts current design principles for metallic implants, which should designed to prevent or minimize corrosion and wear. However, the history of metal implants has been always accompanied by corrosion until it was significantly reduced by the introduction of stainless steels in early 1940s. The numerous reports on side effects of corroding metals *in vivo* before stainless steel has been introduced was probably covering some very promising metals and alloys – those based on magnesium and other metal natural trace elements.

METHODS: This lecture will focus on promising clinical applications performed first by physicians trying to cure their patients. Numerous historically reports and images will be provided as prove of the empirical high-tech approach at that time (Fig.1,Fig.2). Just several decades later, these *in vivo* corroding Mg based alloys were re-discovered and largely re-invented. Examples of current Mg implants will be presented (Fig.3). The old reports will be compared to "novel" approaches and the current technological advantage will be critically discussed.

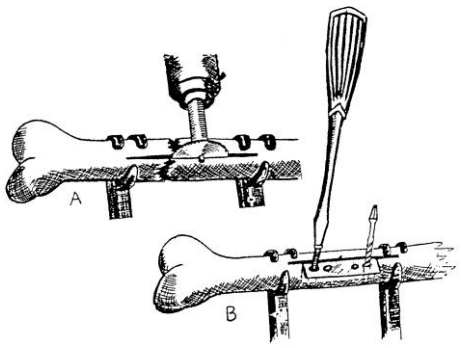

Fig. 1: The physician McBride demonstrated in the year 1938 a method of applying Mg–Mn as a thin angled plate and screws to achieve rotation-resistant osteosynthesis [1].

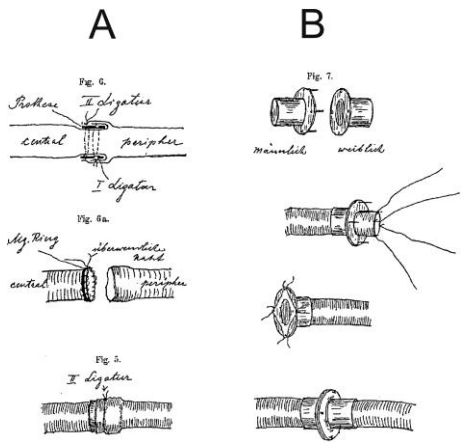

Fig. 2: Tubal Mg connectors designed by Payr in the year 1901 for vessel anastomosis [1]. Method (A) used an extravasal Mg ring, which ensures an open postoperative anastomosis. Method (B) uses a two-part extravasal connector with a male and female part. In both methods the magnesium connector is extravasal and the anastomosis is achieved by a duplication of the intima.

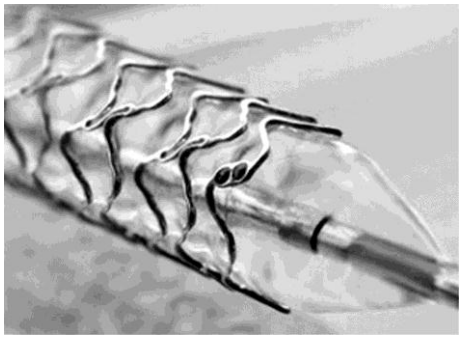

Fig. 3: Current drug-eluting, biodegradable Mg stent from Biotronik (with kind permission).

RESULTS & DISCUSSION: The empirical work of physicians at the bedside of their patients was leading to fundamental observations which are still valid today. However, just lately after focused "bench research" has been performed on this "novel" technology, the dream of biodegradable metal implants is almost accomplished. Current research and development - mainly driven by industry - is very close to complete the empirical development cycle from beside to bench – and finally back into clinic.

REFERENCES: [1] F. Witte (2010) *Acta Biomaterialia* **6**:1680-92.

Epiphyseal chondro-progenitors exhibit spontaneous chondrogenesis in photoencapsulating polyethylene glycol dimethacrylate hydrogels

A Khoushabi[1], SE Darwiche[1,2], P Abdel-Sayed[1], LA Applegate[2], DP Pioletti[1]

[1]*Laboratory of Biomechanical Orthopedics, Ecole Polytechnique Fédérale de Lausanne, CH,* [2]*Unit of Regenerative Therapy, Service of Plastic and Reconstructive Surgery, Centre Hospitalier Universitaire Vaudois, Lausanne, CH*

INTRODUCTION: Articular cartilage possesses a limited inherent regenerative capacity and no gold standard currently exists for cell based cartilage therapy. Characterizing the interaction of potentially therapeutic cells with biomaterial substrates remains key in defining a regenerative strategy. As such, this work investigates the chondrogenic potential of a novel cell source, Epiphyseal Chondro-Progenitors (ECP), embedded in a biologically inert hydrogel. Photopolymerized Polyethylene Glycol Dimethacrylate (PEGDM) hydrogel systems have been widely documented for chondrocyte 3D encapsulation and provide a first step to better tailor the behavior of ECPs embedded in a 3D microenvironment.

METHODS: Various hydrogel formulations were produced using combinations of PEGDM molecular weights (6 kDa and 20 kDa) and concentrations (10%, 20% and 30% w/w). PEGDM photopolymerization was induced under 365nm UV light (~ 4 mW/cm^2) for 10 min using Irgacure® 2959 as a photoinitiator. Cell-free hydrogels were characterized by swelling studies and unconfined axial compression tests. ECPs were encapsulated in hydrogels at a concentration of 5 x 10^6 cells/mL and placed in basal media. Viability was assessed by performing a live/dead stain at 4, 7 and 21 days following encapsulation and the MTS based cell titer assay was used to quantify metabolic activity. The presence of chondrogenic markers such as Sox9, Aggrecan, Glycosaminoglycans, Collagen Type II, Cartilage Oligomeric Matrix Protein, and link protein was assessed by evaluating gene expression and matrix deposition following 21 days of culture in free swelling conditions.

RESULTS: A wide range of stiffness and swelling ratio were obtained across hydrogel formulations (Fig.1), enabling the evaluation of ECP responses to microenvironments with various physical properties. Hydrogels with 10% w/w PEGDM showed the highest cell metabolic activity and viability up to 21 days, with ECPs remaining viable in hydrogels up to 20% w/w PEGDM (Fig.2). Spontaneous pericellular glycosaminoglycan deposition was observed in hydrogels with 10 and 20% w/w PEGDM (Fig.2), with the former showing a more diffuse deposition pattern. An increase in gene expression levels of chondrogenic markers across 10% and 20% w/w hydrogel formulations was also observed. This indicated that the 3D encapsulation in a biologically inert hydrogel was sufficient for ECPs to exhibit inherent chondrogenic properties without the need for chondrogenic morphogen supplementation.

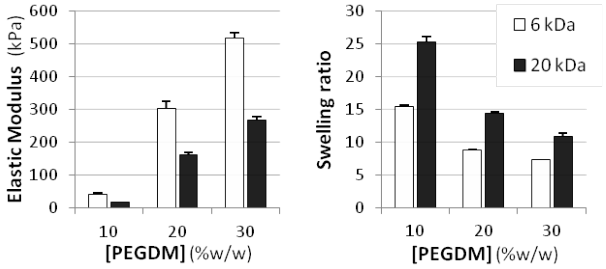

Fig. 1: Elastic modulus (left) and swelling ratio (right) of various PEGDM hydrogel formulations.

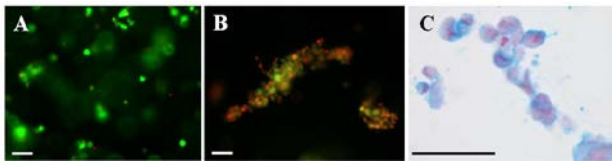

Fig. 2: Viability/Cytotoxicity of ECPs encapsulated in 10% w/w 6 kDa PEGDM (A) and 30% w/w 20 kDa PEGDM (B) after 21 days. Deposition of Glycosaminoglycan (blue) around ECPs (pink) embedded in 20% w/w 20 kDa PEGDM (C). Scale bars indicate 50 µm.

DISCUSSION & CONCLUSIONS: The use of a PEGDM hydrogel system was successful in facilitating the systematic analysis of ECP behavior in relation to finely tuned 3D substrate physical properties. These results mark a first but fundamental step towards designing a biomaterial carrier system to deliver ECPs in vivo.

ACKNOWLEDGEMENTS: These studies were funded by the Swiss National Science Foundation (No. 205320 132809), the Center for Translational Biomechanics EPFL-CHUV-DAL and in part by the Sandoz and S.A.N.T.E Foundations.

A new single step synthesis for thermoresponsive hyaluronan hydrogels

M D'Este, M Alini, D Eglin

[1] *AO Research Institute, AO Foundation, Davos, CH.*

INTRODUCTION: Thermoresponsive hyaluronan hydrogels have been proven to be suitable matrices for nucleus pulpous cells encapsulation *in vitro* [1]. Here we present a convenient synthetic route to the conjugation of amphiphilic thermoreversible polymers to hyaluronic acid (HA). The synthesis resulted effective for the grafting of polyoxyalkyleneamines and poly(N-isopropylacrylamide) (pNIPAM) to HA. The thermoresponsive hydrogels can be used as drug delivery systems, or combined with cells or bioactive ceramics to be used in tissue engineering protocols.

METHODS: Amino terminated pNIPAM (pN-NH_2) of Mw=20kDa was synthesised via living polymerization; Jeffamines® were kindly provided by Huntsman LLC. pN-NH_2 and Jeffamines® were subsequently grafted to HA via amidation chemistry in organic medium using carbonyl diimidazole as condensing agent. Products were purified via exhaustive dialysis and freeze dried. Characterization was performed via ^{1}H NMR, FT-IR, Rheology, and Differential Scanning Calorimetry.

RESULTS: The synthetic route was effective and reproducible. The conjugates with Jeffamine® M-600 and pNIPAM (HApN) displayed improvement of viscoelasticity upon temperature increase. HApN with a degree of substitution of 6.5 ± 1.0 % in moles (calculated from ^{1}H NMR) presented wider transition in a tighter temperature range. Solutions of the conjugate in PBS display opposite behaviour compared with underivatized HA at the same concentration, giving viscoelasticity 4 orders of magnitude lower. Such dramatic decrease is attributed to the amphiphilic moieties of pNIPAM hindering the interactions between the HA chains. Conjugates display a sharp increase of viscoelasticity upon temperature increase above 30°C. Interestingly the profile of the transition was independent on the MW of the HA backbone in the range 0.28-1.64 MDa (fig 1). Such a feature confirms that the structure of the gel is supported by the reversible non-covalent interaction between the pNIPAM moieties rather than dynamical interactions among the HA chains in solution [2].

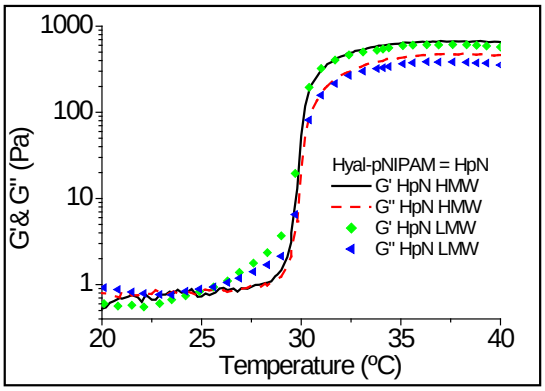

Fig. 1: Temperature dependence of storage and loss moduli of 10% w/w HApN solutions in PBS from High Molecular Weight (HMW, 1.64MDa) HA and Low Molecular Weight (LMW, 0.28MDa) HA

DISCUSSION & CONCLUSIONS: A convenient route to the grafting of amphiphilic polymers to hyaluronic acid is presented. The method is versatile and scaling-up ready, as demonstrated by the conjugation of pN-NH_2 and Jeffamines®. HApN, which displayed the best performance, is currently under investigation as controlled release system for drugs and biologics, as hydrogel biomaterial in cell therapy protocols and as matrix for osteoconductive bio-ceramics.

REFERENCES:

[1]M. Peroglio et al (2012) *Eur Spine Journal* In Press. [2]H. Tim (2004). Chapter 1 - Solution Properties of Hyaluronan. In *Chemistry and Biology of Hyaluronan*, Hari, G. G., Ph.D., D.Sc, Charles, A. H., Eds.; Elsevier Science Ltd: Oxford, pp 1-19.

ACKNOWLEDGEMENTS: Huntsman LLC for the supply of Jeffamines. C. Boissard and PE Bourban (EPFL, Lausanne) and D Sutter (ETH, Zürich) for the rheology and NMR measurements, respectively. M Glarner for support in the syntheses. The research leading to these results has received funding from the European Union's 7th Framework Programme under grant agreement n° NMP3-SL-2010-24.

Proliferation rate as an indicator for the chondrogenic potential of mesenchymal stromal cells in 3D pellet culture

Deborah Studer[1,2], Marcy Zenobi-Wong[2], Katharina Maniura-Weber[1]

[1] Laboratory for Materials-Biology Interactions, Swiss Federal Laboratories for Materials Testing and Research, St.Gallen, CH. [2] Laboratory of Cartilage Engineering and Regeneration, Department of Health, Science and Technology, ETH Zürich, CH.

INTRODUCTION: There is a high interest in adult multipotent mesenchymal stromal cells (MSCs) for their potential therapeutic application in cartilage tissue engineering, where they represent an attractive alternative to chondrocytes, which are limited in number and de-differentiate during expansion. The human body is a source of different MSCs, each exhibiting varying differentiation potential with high interpatient variability. We present the chondrogenic differentiation potential of different MSC donors and sources (derived from bone marrow, placenta and adipose) in 3D pellet culture and how their differentiation potential can be estimated based on their cell index.

METHODS: MSCs were cultivated on tissue plastic and their proliferation rate assessed by impedance measurements (XCelligence, Roche) over 7 days, displayed as Cell Index values that increase with higher proliferation, cell attachment and morphology. This data is complemented with population doubling analysis over 7 days. Later, chondrogenic differentiation was performed in pellet cultures in the presence of TGF-β3, BMP-2 and dexamethasone. Briefly, 250,000 cells were centrifuged at 250g for 5 minutes and cultivated over 14 days. The glycosaminoglycan (GAG) content and gene expression of Collagen II and aggrecan were determined as a read-out for chondrogenesis.

RESULTS: Collagen II expression varies between different MSC sources (Fig. 1) and donors (Fig. 2) showing a correlation with the cell index in tissue culture prior to chondrogenic induction. The higher the Cell Index, the lower the collagen II expression of the chondrogenic pellets.

DISCUSSION & CONCLUSIONS: We propose that the Cell Index is inversely proportional to the degree of differentiation and may be predictive of the chondrogenic potential of the MSCs. This indicator is of high importance for the clinical application of MSCs for cartilage tissue engineering for which a prediction of the success of a cartilage therapy in different patients would be important.

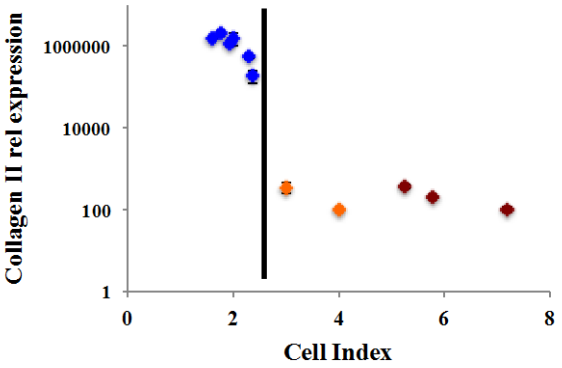

Fig. 1: Negative correlation between collagen II expression and Cell Index of placenta (red), adipose (orange) and bone marrow (blue) derived MSCs at day 14 in pellet culture normalized to day 1. Black line indicates the drop in collagen II expression upon increase in Cell Index

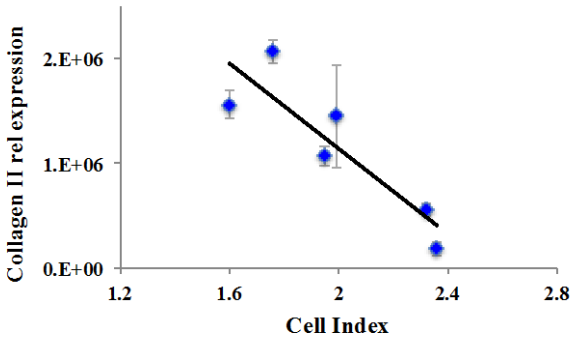

Fig. 2: Collagen II expression of three bone marrow MSC donors after 14 days in pellet culture normalized to day 1 versus the corresponding Cell Index. The black line indicates the linear correlation between Cell Index and collagen II expression.

ACKNOWLEDGEMENTS: This work was supported by the Swiss National Science Foundation (Grant CR23I2_130678)

Degradation of fibrin gels during monoculture of human MSCs

P Lezuo[1], M Alini[1], M Stoddart[1]

[1] *AO Research Institute, AO Foundation, Davos, CH.*

INTRODUCTION: Fibrin gels are frequently used to embed human bone marrow derived mesenchymal stem cells (MSC's) for their maintenance and expansion *in vitro*. However, an inhibitor is required to prevent the degradation of fibrin and release of the cells. In the case of a perfusion bioreactor this would have the potential to block the perfusion of the device. This study aimed to determine the optimal concentration of ε-aminocaproic acid to prevent the degradation of low concentration fibrin gels in the presence of human MSC's.

METHODS: Human MSC's (5 mio/gel, Ø 8.1 x 5.1 mm) from three different donors were embedded into low concentration fibrin gels (5 mg/ml Fibrinogen, 2 IU/ml of Thrombin). In smaller, other than 5 mio/gel of hMSC's or fibrin gel (5 mg/ml of Fibrinogen and 2 IU/ml Thrombin) were tested as well.

During the three month's culture period every third day the culture medium was changed with fresh culture medium (DMEM plus 10% FCS and different concentrations of ε-aminocaproic acid ($1.4\cdot10^{-5}$, $2.1\cdot10^{-5}$, $2.9\cdot10^{-5}$, $4.3\cdot10^{-5}$, $6.4\cdot10^{-5}$ M)).

RESULTS: At the concentration of ε-aminocaproic acid below $2.1\cdot10^{-5}$ M, the gels immediately started to degrade and releasing hMSC's into the culture well plates. At the concentration of $2.9\cdot10^{-5}$ to $4.3\cdot10^{-5}$ M, there was a significant reduction in fibrin gel degradation, whereas concentrations of ε-aminocaproic acid above $4.3\cdot10^{-5}$ M resulted in the release of few hMSC's into the culture media. However, at concentrations above $6.4\cdot10^{-5}$ M ε-aminocaproic acid a 95% reduction in proliferation was observed. In experiments other than standard cell density or fibrin gel composition, there resulted in shrinkage of the fibrin gels from their initial size. At 2.5 mio/gel of hMSC's in 5 mg Fibrinogen and 2 IU/ml Thrombin the fibrin gel was completely enveloped by hMSC's after a few days in culture, so that the surrounding cell layer at the surface was visible under the microscope, resulting in a limited degradation of the fibrin gel.

Finally there was also an important donor dependent influence on fibrin gel degradation. hMSC's from three different donors showed varying levels of metabolic and proliferative activities, which led to a faster or lower degradation of the fibrin gels. This led to a higher or lower concentration of ε-aminocaproic acid in the culture medium as determined in this investigation.

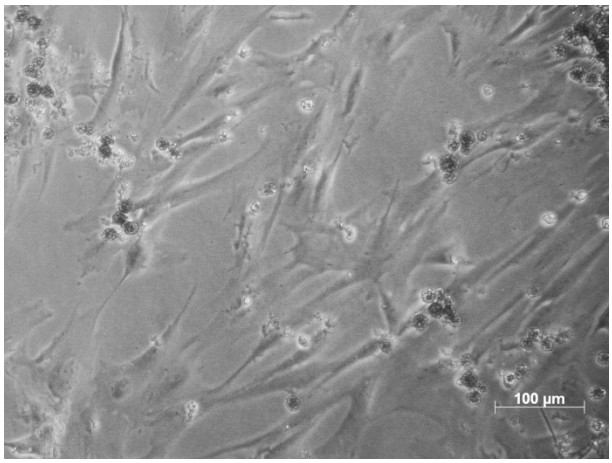

Fig. 1: Image of fibrin gel embedded hMSC's attached to spread hMSC's on the bottom of well plate.

DISCUSSION & CONCLUSIONS: In these experiments we could determine that the optimal concentration of ε-aminocaproic acid to prevent fibrinolysis of fibrin gels over a three month time period were between $2.9\cdot10^{-5}$ to $4.4\cdot10^{-5}$ M. A small range of uncertainty remains due to differences between different donor metabolism and proliferation behaviour.

REFERENCES: [1] I. Catelas et al. (2006) *Tissue Eng* **12**:2385-95. [2] D. Pelaez et al. (2009) *Stem Cells Dev* **18**:93-102. [3] W. Ho et al. (2006) *Tissue Eng* **12**:1587-1595. [4] C.R. Lee et al. (2005) *Tissue Eng* **11**:1562-1573. [5] L. Kupcsik et al. (2009) *Tissue Eng: Part A* **15**:2309-2313. [6] J.W. Weisel et al. (1992) *Biophys J* **63**:111-128.

ACKNOWLEDGEMENTS: Fibrin components were kindly provided by Baxter Biosurgery (Vienna, Austria).

A maturation thresholding process regulates cell adhesion at the distal lamellum

Y Loosli[1,2,3], C Labouesse[4], R Luginbhuel[3], B Vianay[4], JG Snedeker[1,2]

[1] Orthopaedic Research Laboratory, Uniklinik Balgrist, CH,[2]Institute for Biomechanics, ETHZ, Zürich, CH, [3]RMS Foundation, Bettlach, CH,[4] Laboratory of Cell Biophysics, EPFL, Lausanne, CH

INTRODUCTION: How cells interact with their substrate drives adherent cell behavior (growth, migration, cycle, differentiation) and understanding these interactions is critical in the choice of scaffolding material. The mechanical coupling between a cell cytoskeleton and its substrate operates via mature adhesion sites to stable actin bundles, although the mechanisms behind their formation until now remains largely obscure.

The present study provides first experimental confirmation of a mechanism that may govern formation of cell-biomaterial adhesion, a process we dub the Maturation Thresholding Process (MTP). Here remote lamellar myosin II activity acts on actin bundles aligned with the cell leading edge. When bundle length exceeds a given length threshold, the accumulated lamellar forces then become sufficiently large to trigger the stabilization of the bundle and its anchoring adhesions.

METHODS: 3T3 fibroblasts were seeded on adhesive micro-patterns fabricated by adsorption of fibronectin by UV-photolithography. Patterns were circular (1000μm^2) with 2, 4, 6, 8 or 10μm non adhesive rectangular gaps (Fig.1). Fluorescence imaging (63x) of actin and vinculin revealed actin filament and adhesion site layout. These image channels were visually inspected to identify stable actin bundles aligned with the cell front and terminated by two adhesions. Of these stable actin bundles, those spanning non-adhesive gaps were designated as actin bridges (ABs). According to the MTP, we expected ABs to systematically form on engineered substrates with non-adhesive gaps larger than the MTP threshold. We computed the ratio of bridged gaps to the total number of gaps beneath the cell, with ratios for cells spread on identical patterns averaged and presented as a function of pattern gap width.

RESULTS: Cells established ABs with lengths generally exceeding the imposed gap width (Fig. 1). From 65 analysed cells, 430 gaps were covered and 246 ABs were detected allowing a statistically meaningful analysis. The bridging ratio increased with increasing non-adhesive gap width (from 30% for the 2μm pattern to 100% for gaps wider than 8μm; Fig.1). The standard deviation of the bridging ratio, corresponding to variability in bridging behavior, was maximal on 4μm patterns.

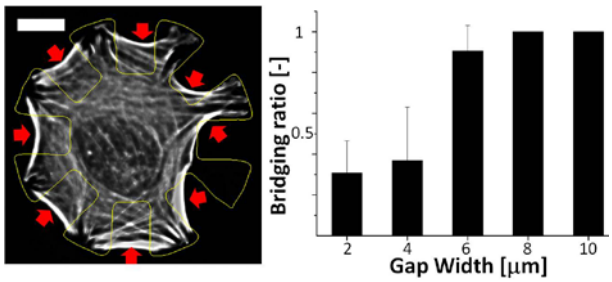

Fig. 1: (Left) Actin cytoskeleton of a cell spread on 10μm pattern (yellow line) with systematic ABs occurrence (arrows point ABs); bar 10μm. (Right) Bridging ratio vs. non-adhesive gap width indicates a threshold between 4 and 6 μm.

DISCUSSION & CONCLUSIONS: While actin bridges occurred on all patterns (including those with small non-adhesive gaps), lengths of the ABs detected on the small patterns were nearly all above 4μm (results not shown). Further, bridging ratio increased step-wise as gap increased from 4 to 6μm, indicating a substrate dependent behavioural switch. These combined observations point strongly to a MTP with a threshold above 4μm. The increased bridging variability observed on the 4μm gap patterns further indicates that the switch may be closer to 4 than 6μm, corroborating the consistently observed AB lengths above 4μm.

We were thus able to experimentally demonstrate the existence of a threshold mechanism that triggers adhesion maturation and actin bundle stabilization. We further provide a first estimate for a thresholding length of approximately 4.5μm. This "Maturation Thresholding Process" may be critical in the design of cell-instructive biomaterials with enhanced cellular adherence.

Resorbable ceramic platelets for reinforcement of bone substitutes

L. Galea[1], M. Bohner[1], O. Loeffel[1], S. Gruenenfelder[1], M. Niederberger[2], T. Graule[3]

[1] *RMS Foundation, Bettlach, CH* [2] *ETHZ, Zurich, CH* [3] *EMPA, Dübendorf, CH*

INTRODUCTION: Calcium phosphate (CaP) ceramics are widely used as bone graft substitutes [1]. β-tricalcium phosphate (β-TCP) is of particular interest because it is biocompatible, has a chemistry close to that of the mineral part of bone and is actively resorbed by osteoclasts. β-TCP is usually obtained by high temperature processes [1]. Hence, the particles are agglome-rated, have undefined shapes and broad size distri-butions. Their potential use is thus limited, espe-cially as reinforcement in composite where mono-disperse, non-agglomerated platelets with well-defined shape and size are needed to build well organized structures with high ceramic content [2]. Recently, the synthesis of hexagonal β-TCP single crystals by precipitation in ethylene glycol at a relatively low temperature (150°C) was reported [3]. The effects of temperature and concentration on crystal morphology and crystallinity were briefly investigated, but no attention was paid to crystal size (diameter, d, and thickness, h) and aspect ratio (s=d/h). The aim of this study was to better understand the β-TCP crystallization process and to find ways to tune the size and aspect ratio of the particles. In particular, the influence of reaction time, Ca^{2+}, PO_4^{3-} and Mg^{2+} ions concen-tration were investigated. Griffith's criterion and modified rule of mixture equations were used to determine the ideal platelets size and aspect ratio to reinforce efficiently an organic matrix [2].

METHODS: A Na_2HPO_4 ethylene glycol solution was added to a $CaCl_2$ ethylene glycol solution at 150°C. Different concentrations ($[Ca^{2+}+PO_4^{3-}]$= 1.5/15/30mM) were used. Mg^{2+} ions were added to the Ca-solution (0-1mol%). After 24h under intense stirring, the solution was cooled down in air and rinsed using centrifugation steps in ethanol and demineralised water. The time influence was studied by taking out a few mL of the 15mM solution at regular intervals. The crystalline composition was determined by XRD and the size and aspect ratio of the particles were measured by image analysis of SEM images.

RESULTS & DISCUSSION: During the first seconds of the reaction, only a gel-looking phase was observed, possibly amorphous CaP [3]. A few small hexagonal platelets were observed from 30s, growing linearly with time to reach d= 600-850nm and h=125-170nm at 2min. Later, the amorphous phase disappeared, but the size did not increase anymore. The size and aspect ratio of the platelets can thus not increase indefinitely with the reaction time. The particles size and aspect ratio increased with increasing Ca^{2+} and PO_4^{3-} ions concentration but remained below d=1μm and s=6. The presence of Mg^{2+} ions decreased the size and aspect ratio of the crystals down to d≈130nm and h≈44nm with 1mol% of Mg^{2+} ions. This emphasises the need for Mg-free chemicals if large particles with a high aspect ratio are desired. Indeed, Mg^{2+} ions are often present as impurities in $CaCl_2$. In all conditions, the platelets size dispersion was very narrow (SD/mean<0.10, Fig. 1a). According to XRD, these platelets consisted of β-TCP.

According to Griffith's law, platelets thinner than 300nm should reach the intrinsic strength of β-TCP. To obtain the maximum reinforcing effect without brittle fracture of the composite s should be just below 20. For bone substitute application, the strength of the composite should be similar to the properties of cortical bone, i.e. σ_t≈150MPa and a toughness of a few MPa*$m^{1/2}$. The platelets obtained here are thus thin enough, but the limited aspect ratio (<6), restricts the prospective strength of a theoretical composite structure (Fig. 1b).

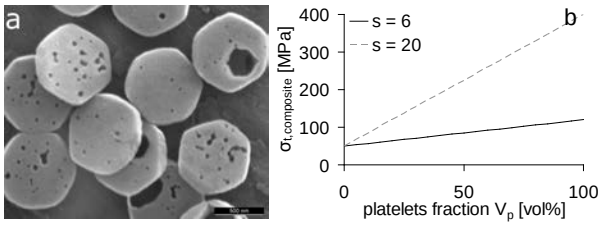

Fig. 1: (a) Typical β-TCP platelets (scale bar = 500nm) (b) Strength of a theoretical composite in function of aspect ratio, s, and platelets fraction.

CONCLUSIONS: The reaction time, the presence of impurities (Mg^{2+}) and the concentration of Ca^{2+} and PO_4^{3-} ions influence the size and aspect ratio of β-TCP platelets, but these effects are limited, restricting the potential reinforcing effect of the platelets.

REFERENCES: [1]R.Z. LeGeros (2002) *Clin Orthop* **395**:81-98. [2]L. Bonderer et al (2008) *Science* **319**:1069-1073. [3]J. Tao et al (2009) *Cryst. Growth Design* **9(7)**:3154-3160.

Vitamin E stabilised, cross-linked UHMWPE: Leaching out of vitamin E?

R. Lerf [1], D. Delfosse [1], D. Zurbrügg [2]

[1]*Innovation & Technology, Mathys Ltd Bettlach, Bettlach,* [2]*Niutec AG, Winterthur, Switzerland*

INTRODUCTION: Vitamin E stabilised, highly cross-linked UHMWPE is commercially available as articulating parts of joint replacement by several orthopaedic manufacturers. Such PE implants have low wear rate due to cross-linking and increased oxidative stability due to the addition of vitamin E. Although the stabilising effect of vitamin E is undisputed, the physical and chemical state of vitamin E in cross-linked UHMWPE is still under investigation. On the one hand, it was found that migration of vitamin E out of the polymer is unlikely [1]. On the other hand, grafting of vitamin E molecules to the polyethylene backbone was postulated [2]. The purpose of this investigation is to elucidate the amount of vitamin E leachable out of the PE and evaluate the chemical nature of the vitamin E remaining in the PE.

METHODS: Pre-forms were sintered of UHMWPE powder GUR 1020 blended with two differ-ent concentrations of vitamin E (0.1 wt % and 1.0 wt %). A sample of each was kept in the "as sintered" condition, whereas those for cross-linking were packaged under vacuum and irradiated by g-rays at a dose of 96.5 kGy. The 0.1 % material corresponds to vitamys® UHMWPE by Mathys Ltd Bettlach used hip cups. For comparison, an E-Poly sample by Biomet (E-Poly liner Ringloc-X by Biomet, size 66/36) was investigated, too. To assess the extent of vitamin E leachable out, three 0.3 mm sections were cut from the centre of all samples. These PE films were extracted for 48 h in heptane at 98 °C and finally dried at room temperature. The amount of vitamin E in the PE was analysed by Fourier transform infrared spectroscopy (FTIR). The vitamin E index (VEI) was calculated as the ratio of the area of a characteristic vitamin E peak (1275 -1245 cm^{-1}) to the polyethylene reference peak at 1985-1850 cm^{-1} and the relative vitamin E index (RVEI) was calculated by subtracting the background of a pure UHMWPE.

RESULTS: There is a marked disparity in the amount of vitamin E extracted in the as sintered and the cross-linked state. Vitamin E of the non-irradiated samples is completely extracted. After extraction, RVEI of both samples is below the detection limit of 0.001. Besides cross-linking, an effect of irradiation is the at least partial bonding of vitamin E to the polymer. These grafted molecules of anti-oxidant can no longer be extracted. The extracted amount of vitamin E is 23 % for the 0.1 % vitamys® sample and reaches 87 % in the experimental 1.0 % material. From the E-Poly liner, 95 % could be extracted.

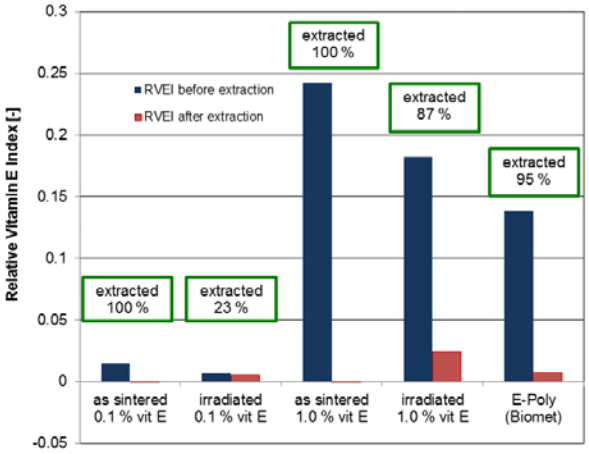

Fig. 1: Relative vitamin E index (RVEI) before and after extraction, measured by FTIR. The percentage of decrease in RVEI is indicated for each sample.

DISCUSSION & CONCLUSIONS: The amount of vitamin E remaining in the polymer is not proportional to the initial concentration. It seems rather that there is a saturation of the absolute amount of vitamin E grafted for a given dose of irradiation. The grafting of the anti-oxidant has shown to reduce the amount of vitamin E which can be leached out, while protection of the UHMWPE against oxidation remains high [3]. Under this aspect, blending of vitamin E before irradiation for cross-linking provides a PE stabilised against oxidation and against leaching out of vitamin E.

REFERENCES: [1]E. Oral et al (2006) *Biomaterials* 27:2434-2439. [2]C. Wolf et al., ORS 2011 Annual Meeting, poster 1178. [3]R. Lerf et al (2010) *Biomaterials* 31:3643–3648

Covalent conjugation of bone morphogenetic protein-2 in fibrin hydrogels with cell-determined release for intervertebral disc regeneration

LS Karfeld-Sulzer[1], C Ghayor[1], FE Weber[1]

[1] *Division of Cranio-Maxillo-Facial and Oral Surgery, University Hospital Zurich, Zurich, CH.*

INTRODUCTION: Degenerative disc disease is characterized by the breakdown of proteoglycans and matrix proteins, especially in the inner part of the intervertebral disc (IVD), called the nucleus pulposus (NP), leading to a decreased disc height. The NP cannot properly perform its stress transfer functions, resulting in back pain. Several growth factors, including bone morphogenetic protein-2 (BMP-2), have been shown to increase proteoglycan and collagen content in disc cells. Studies have indicated that a proper extracellular matrix environment and growth factor administration can induce reversal of disc degeneration [1]. Considering that growth factors have extremely short in vivo circulation times, the importance of extended exposure [2] and the desire to avoid heterotopic ossification outside of the disc, we have explored enzymatic, covalent incorporation of BMP-2 into fibrin, a pertinent component of the wound healing cascade that has been shown to support NP cells [3, 4]. The tethered BMP-2 can be retained in the matrix until released by cells through an included plasmin-cleavable site.

METHODS: Recombinant human BMP-2 and a modified BMP-2 including amino acids for transglutaminase crosslinking and plasmin cleavage (TG-BMP-2, with the TG indicating the transglutaminase enzymatic crosslinking site), were cloned and expressed in *E. coli*. Monomers were purified with affinity and size exclusion chromatography, refolded in a buffer with CHAPS and glutathione, and dimers were separated from any unfolded growth factor. Both BMP-2 and TG-BMP-2 were included in fibrin gels formed with fibrinogen, thrombin, and preactivated Factor XIII. Extracts from hydrogels digested with trypsin or plasmin were assayed on Western blots probed with an anti-BMP-2 antibody. The activity of BMP-2 and TG-BMP-2 were assessed via stimulation of C2C12 cells and subsequent measurement of alkaline phosphatase.

RESULTS: An upward shift in mobility of plasmin-digested TG-BMP-2 compared to undigested TG-BMP-2 in a Western blot indicated the functionality of the plasmin cleavage site in TG-BMP-2. A Western blot of trypsin-digested fibrin gels showed a decrease in mobility in SDS gels of TG-BMP-2 compared to a TG-BMP-2 trypsin-digested control. However, BMP-2 in trypsin-digested fibrin gels had the same mobility as the trypsin-digested BMP-2 control. These results indicated that TG-BMP-2 is covalently incorporated. Additionally, released BMP-2 and TG-BMP-2 from trypsin-digested gels were functional, as measured with an alkaline phosphatase assay.

DISCUSSION & CONCLUSIONS: We have demonstrated the functionality of both the plasmin cleavage site and the Factor XIII crosslinking site in the modified TG-BMP-2 growth factor. When TG-BMP-2 is covalently incorporated into fibrin gels and then released by trypsin digestion, it will be attached to some amino acids from the fibrin, increasing the molecular weight. This higher molecular weight is demonstrated by the decrease in mobility on an SDS gel, confirming the covalent conjugation. Thus, we have demonstrated that TG-BMP-2 can be covalently integrated into fibrin gels. The alkaline phosphatase activity of released TG-BMP-2 and BMP-2 from trypsin-digested gels indicated that these growth factors are still functional after incorporation into the gel. These findings indicate the potential of this growth factor delivery system for IVD regeneration.

REFERENCES: [1] H.S. An, K. Takegami, H. Kamada, et al (2005) *Spine* **30**:25-31. [2] Y. Imai, K. Miyamoto, H.S. An, et al (2007) *Spine* **32**:1303-1309. [3] H. Bertram, M. Kroeber, H. Wang, et al (2005) *Bioch Biophys Res Comm* **331**:1185-1192. [4] S. Stern, K. Lindenhayn, O. Schultz, et al (2000) *Acta Orthop Scand* **71**:496-502.

ACKNOWLEDGEMENTS: The authors gratefully acknowledge the support of the European Project: NP Mimetic - Biomimetic Nano-Fiber Based Nucleus Pulposus Regeneration for the Treatment of Degenerative Disc Disease, funded by the European Commission under FP7 (grant NMP3-SL-2010-246351).

Novel Resorbable Calcium Phosphate Putty for Bone Tissue Engineering

Charles Sfeir[1,2,3], Abhijit Roy[1,2,3], Samer Zaky[1,2,3], Sayuri Yoshizawa[1,2,3], Bernard Costello[3,4], Prashant N. Kumta[1,2,3],

[1]Center for Craniofacial Regeneration, [2]Department of Bioengineering , [3]McGowan Institute for Regenerative Medicine, [4]Department of Oral and Maxillofacial Surgery, University of Pittsburgh, Pittsburgh, PA, USA

INTRODUCTION: There has been significant research in the development of polymer and ceramic cement based scaffolds for bone tissue engineering. However, most of these systems are not amenable for in situ incorporation of cells, growth factors and/or biological systems.

There is a need to develop safe and effective craniofacial/orthopedic bone regeneration material. The objective of this study is to determine the efficacy of a novel biodegradable nano-structured Calcium Phosphate (CaP) based putty for bone regeneration. This putty will contain nano-sized CaP nanoparticles (NanoCaPs) [1,2], as carriers, with or without BMP-2 to enhance bone regeneration in a critical sized bone defect model.

METHODS: Nano-structured porous calcium phosphate based putty carrying nanosized CaPs nanoparticles (NanoCaPs) were prepared and characterized prior to their *in vivo* use. Critical size defects (CSD) in rabbit ulnae (1.5-cm segmental defect) and a 15mm diameter rabbit craniofacial defect were created to test the regeneration potential of the putty alone or with BMP-2. X-rays were taken immediately following the surgery as well as 2, 8 and 26 weeks post-op. Rabbit specimens were harvested at designated time points and Micro-CT as well as histological, and histomorphometry analysis were performed to quantify bone regeneration.

RESULTS: The putty shows excellent cell attachment and cellular migration. The nanostructured nature and the high specific surface area of the HA formed as a result of the setting reaction are added factors contributing to the likely observed faster resorption kinetics of the implanted putty. Our results of the radiographical, micro-CT and histological assessment of the new regenerative bone (Figure 1) showed that with or without BMP-2 addition to the CaP-putty yielded higher bone regeneration compared to the control groups.

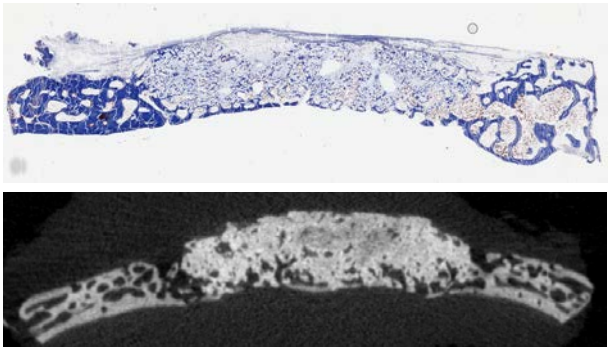

Fig. 1: Rabbit critical size defect implanted with bone putty alone and assessed at six months for bone regeneration

DISCUSSION & CONCLUSIONS: The putty shows excellent cell attachment and cellular migration. The nanostructured nature and the high specific surface area of the HA formed as a result of the setting reaction are added factors contributing to the likely obsereved faster resorption kinetics of the implanted putty. Our results of the radiographical, micro-CT and histological assessment of the new regenerative bone showed that with or without BMP-2 addition to the CaP-putty yielded higher bone regeneration compared to the control groups.

REFERENCES:

[1]D. Olton et al (2007) *Biomaterials* **28**:1267. [2]P. Kumta et al (2005) *Acta Biomater* **1**:65–83

ACKNOWLEDGEMENTS: We would like to acknowledge the National Tissue Engineering Center (NTEC), DCED, AFIRM, Center for Craniofacial Regeneration, Univ. of Pittsburgh and the Edward R. Weidlein Chair Professorship funds for supporting this research.

Design of a modular reactor for biofilm formation studies in biomaterials

J. Barros[1,2], C.M. Manuel[4,5], L. Grenho[1,2], F.J. Monteiro[1,2], L. Melo[2,4], O.C. Nunes[2,4] and M.P. Ferraz[1,3]

[1] INEB - Instituto de Engenharia Biomédica, [2]FEUP - Faculdade de Engenharia, Departamento de Engenharia Metalúrgica e Materiais, [3]CEBIMED - Centro de Estudos em Biomedicina Universidade Fernando Pessoa, [4]LEPAE – Laboratory for Process, Environmental and Energy Engineering, Faculty of Engineering, [5]University Lusofona of Porto, Porto, Portugal

INTRODUCTION: Biofilms form on inert or living surfaces and are composed of heterogeneous communities of bacteria functionally organized and enclosed in a self-produced polymeric matrix. Although largely beneficial to human life such as those used in processes in the intestinal tract, in wastewater treatment and in food processing, biofilms present a negative potential of attaching to biomaterials such as in dental and orthopedic devices[1,2]. To control this problem, implant surfaces have been developed in order to minimize the bacterial adhesion and biofilm formation [1,2]. Prior to the implementation in real medical devices, these new surfaces must be initially tested in laboratory reactors in which biofilms are grown under conditions mimicking those observed inside the human body [3.] In this study, the objective was the setup of a reactor to evaluate biofilm formation to test new developed antibacterial surfaces with reproducible results.

METHODS: The bacterium used in this study was *Staphylococcus epidermidis* RP61A chosen as the most commonly found in orthopaedic infections. Disks of nanoHA of 8,16 mm diameter were prepared by pressing and sintered for 15 min at 1000ºC. The modular reactor was cleaned, sterilized and nine disks of nanoHA were placed inside (*fig 1*). The reactor operated under a continuous flow of a staphylococcal suspension with ca. 10^8 cell/ml, at 37ºC and 0,925 ml/min. The modular reactor was operated for 12 and 24 hours and the disks with the adhered biofilm were collected and tested in triplicates. The total, metabolic active and cultivable cells per unit surface area, and the biofilm coverage rate were assessed by EF microscopy. The surface structures of the formed biofilms were observed by SEM.

RESULTS: *S. epidermidis* RP61A formed a biofilm well dispersed in nanohydroxyapatite disks with 6.33×10^6 cells/mm^2, from which 25,3% and 31.4% were metabolically active and cultivable, respectively after 12 h of operation**.** The biofilms formed after 24h had much more expolymers surrounding the bacteria than those formed in 12h of operation (*fig 1*).

Fig. 1: Photograph of the experimental system used to perform biofilm formation on the reactor. And SEM micrographics of biofilms grown on nanoHA disks collected at 30000 magnifications, with a working distance of 10 mm and an x-ray energy of 15 kV. Where a mature biofilm embedded in an extracellular matrix was observed.

DISCUSSION & CONCLUSIONS: The resulted indicated that *S.epidermidis* RP61A formed a biofilm well dispersed in nanohydroxyapatite and the results of the different measured parameters were reproducible. The different measured parameters were reproducible and the reactor is suitable for biofilm studies.

REFERENCES: [1]Vieira et al (1999) *Biopr Eng.* **20**:369-375. [2]Kajiyama et al (2009) *J Orthop Sci*, **14**:769-775. [3]Williams et al (2010) *Microsc Microanal*, **16**:143-152.

ACKNOWLEDGEMENTS: This work was financed by FEDER funds through the *Programa Operacional Factores de Competitividade* – COMPETE and by Portuguese funds through FCT in the framework of the project NaNOBiofilm (PTDC/SAU-BMA/111233/2009).

Influence of microstructured and nanostructured hydroxyapatite surfaces on human osteoclast differentiation and activation

S Carmo[1,2], J Costa-Rodrigues[1], FJ Monteiro[2], MH Fernandes[1]

[1] Laboratório de Farmacologia e Biocompatibilidade Celular, Faculdade de Medicina Dentária, Universidade do Porto, Portugal [2] Faculdade de Engenharia, Universidade do Porto, Portugal

INTRODUCTION: The bone tissue has an extracellular mineralized matrix, composed essentially by hydroxyapatite (HA). Due to this, synthetic hydroxyapatite appears as a potentially good biomaterial for bone regeneration applications because it displays good bioactive and osteoconductive properties[1]. Nevertheless, it presents a slow resorption rate and its mechanical characteristics are not always suitable for the proposed applications. In order to improve their biological properties and with the advent of micro- and nanoscale technology, nanostructured HA (nanoHA) is being increasingly studied and applied, revealing a high potential in many bone regeneration applications. Nanoscaled materials display improved performances due to their large surface to volume ratio and especially to their surface reactivity (unusual chemical/electronic synergistic effects). In particular, the properties of nanoHA as compared to microphased HA (microHA), such as surface grain size, pore size and wettability may control protein interactions (like adsorption, conformation and bioactivity) and thus interfere with cellular responses[1,2]. This potential to modulate the cellular behavior has generated a landslide of research with nanoscaled biomaterials in the orthopedic field. In this work, the behavior of osteoclastic cells cultured over nanoHA and microHA disks was evaluated and compared.

METHODS: NanoHA (sintered at 830ºC and 1000ºC, nanoHA830 and nanoHA1000, respectively) and microHA (sintered at 1300ºC, microHA1300) disks were characterized by scanning electron microscopy, atomic force microscopy, X-ray diffraction, Fourier transformed infrared spectroscopy and contact angle analysis. Osteoclast precursors (PBMC) were isolated from human peripheral blood as described before[3] and seeded over the biomaterials. When indicated, cultures were treated with inhibitors of MEK, NFkB, PKC, p38 and JNK signaling pathways. Cell cultures were maintained either in the absence of osteoclastogenic enhancers (base medium) or in the presence of recombinant M-CSF and RANKL, and were assessed at days 14 and 21 for tartarate-resistant acid phosphatase activity, presence of cells with actin rings and expressing vitronectin and calcitonin receptors, and ability to resorb HA.

RESULTS: It was observed that nanoHA830 and nanoHA1000 disks displayed surface characteristics distinct of each other and of microHA, with an average grain size of about 70 nm, 150 nm and 3 μm, respectively. The osteoclastogenic behavior of cell cultures maintained in base medium was not significantly affected by the different HA surface properties. On the other hand, important differences were noted in the presence of M-CSF and RANKL, observed not only in cellular differentiation but also in osteoclast HA resorbing ability. Furthermore, the intracellular mechanisms involved in the cellular response appeared to be dependent on the different HA characteristics.

DISCUSSION & CONCLUSIONS: In conclusion, osteoclastogenesis is influenced by the surface properties of HA, such as, for example, its grain size. An understanding of how this modulation occurs can open the possibility to design new biomaterials to be used in bone tissue regeneration strategies.

REFERENCES: [1] S.J. Kalita, A. Bhardwaj, H.A. Bhatt (2007) *Mater Sci Eng C* **27**:441–9. [2] R. Murugan, S. Ramakrishna (2005) *Compos Sci Technol* **65**:2385–406. [3] J. Costa-Rodrigues, A. Fernandes, M.A. Lopes, M.H. Fernandes (2012) *Acta Biomater* **8**:1137–45.

ACKNOWLEDGEMENTS: Finantial support by Faculdade de Medicina Dentária, Universidade do Porto, Portugal. CLSM observation was performed at Advanced Light Microscopy, IBMC, University of Porto (IBMC.INEB) under the responsibility of Dr. Paula Sampaio.

Micropatterned bioactive thin films for guided bone regeneration

A Carvalho[1,2], A Pelaez-Vargas[1,2,3], D Gallego-Perez[4], MH Fernandes[5], DJ Hansford[4], FJ Monteiro[1,2]

[1]INEB- Instituto Engenharia Biomédica, Porto, Portugal. [2] Universidade do Porto, Faculdade de Engenharia, DEMM, Porto, Portugal. [3]Universidad Cooperativa de Colombia, Medellín, Colombia, [4]The Ohio State University, Dept. of BME, Columbus (OH), USA. [5]Laboratório de Farmacologia e Biocompatibilidade Celular, Faculdade de Medicina Dentária, Universidade do Porto, Porto, Portugal.

INTRODUCTION: In maxillofacial applications, biomaterials have been used to fill bone defects that result from malformation, trauma or tumor resections [1]. Ideally, the implanted biomaterial should replace the missing bone, but also stimulate osteoconduction for bone re-growth [2]. Several studies using patterned surfaces have shown improved cellular activity and enhancement of extracellular matrix synthesis of adherent cells, providing a faster and more reliable osseointegrative response [3, 4].

METHODS: A combined methodology of sol-gel and soft-lithography was used to produce micropatterned SiO_2 thin films. Spin-coating was used to create a flat silica surface. Materials were characterized by SEM. Both thin films were cultured with human dental-pulp MSCs (hDP-MSCs) under osteogenic conditions at four time-points (1, 7, 14 and 21 days). TCPS was used as control group for all experiments. Cell metabolic and ALP activities were measured at all time points and morphological analysis was carried out by fluorescence microscopy and SEM. Runx-2 gene expression was assessed at days 14 and 21 of culture by rt-PCR.

RESULTS: Anisotropic micropatterned silica thin films with ~5x5 μm lines and ~10 μm interspacing were successfully fabricated. From day 1, MSCs showed an elongated morphology and orientation along the patterns (Fig. 1b). This behavior increased in the subsequent time points, with cell proliferation occurring over all surfaces. Both cell metabolic and ALP activities increased, without significant differences between the thin films. At day 21, SEM micrographs confirmed mineralization on all SiO_2 surfaces (Fig. 1c, d). Runx2 gene was expressed at both 14 and 21 days of culture in all the tested samples, with a higher expression on the patterned surfaces (relative to the flat surfaces) at day 14.

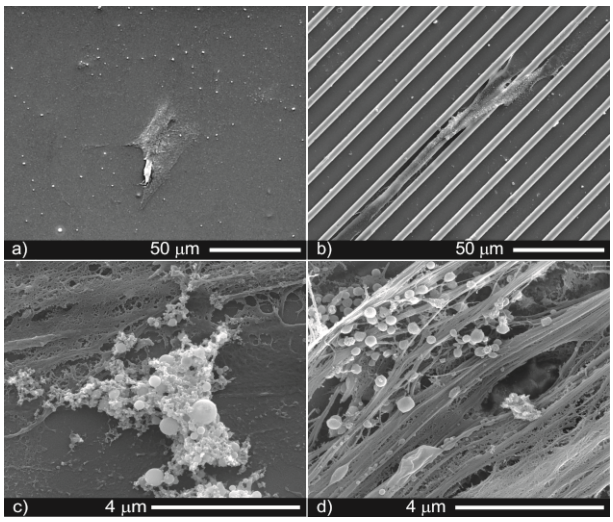

Fig. 1: SEM images of hDP-MSCS at day 1 and 21 on flat surface (a, c) and patterned SiO_2 (b, d).

DISCUSSION & CONCLUSIONS: The micropatterned thin films induced early cell alignment that was maintained through all times of culture, together with good cellular response. hDP-MSCs underwent osteogenic differentiation on all SiO_2 surfaces, as confirmed by ALP activity, Runx2 expression, and mineralization. The higher expression of Runx2 at day 14 in the patterned samples suggests that the osteogenic differentiation may have started earlier on these surfaces.

REFERENCES: [1] A. Neumann (2009) *Laryngorhinootologie* **88** Suppl 1:S48-63. [2] E. Neovius and T. Engstrand (2010) *J Plast Reconstr Aes* **63**:1615-1623. [3] A. Pelaez-Vargas, D. Gallego-Perez, M. Magallanes-Perdomo et al (2011) *Dent Mater* **27**:581-589. [4] G. Mendonça, D. Mendonça, F. Aragão et al (2008) *Biomaterials* **29**:3822–3835.

ACKNOWLEDGEMENTS: The authors acknowledge financial support by FEDER (COMPETE), FCT (PTDC/CTM/100120/2008 "Bonamidi", FCT/SFRH/BD/36220/2007), CRUP E46/09 and MICINN: HP2008-0075.

The effect of micro-porosity on the thermal stability of α-TCP

N Döbelin[1], U Eggenberger[2], M Bohner[1]

[1] *RMS Foundation, Bettlach, Switzerland.* [2] *Institute of Geology, University of Bern, Switzerland*

INTRODUCTION: α-TCP (α-$Ca_3(PO_4)_2$) is used as a raw material in a variety of synthetic bone substitute products due to its reactivity with water and its excellent biocompatibility. It is obtained from calcium phosphate precursors by thermal treatment above 1125 °C[1]. When cooled rapidly, it remains metastable at room temperature without transforming to the less reactive β-TCP phase. Depending on some physical and chemical parameters it can be difficult to avoid partial transformation to β-TCP, though. Some of these critical parameters have not been investigated in detail yet. The aim of this project was to systematically analyze the effect of micro-porosity in solid α-TCP samples on the thermal stability of α-TCP phase.

METHODS: α-TCP cylinders were prepared by mixing pure α-TCP powder with H_2O and casting the slurry into cylindrical moulds. After curing the cylinders were extruded and thermally treated for 4 hours at 1350 °C in order to transform the hydrated phases back to α-TCP. The amount of micro-porosity was controlled by the amount of H_2O in the slurry. Liquid-to-powder ratios (LPR) and porosities are shown in Table 1. A solution of 0.1 % w/v of polyacrylic acid Na salt 5100 (PAA) was used as a wetting agent in one sample to further reduce the LPR and increase the density. The cylindrical α-TCP samples were heated at 900 °C for 2 to 54 hours, which led to a relatively fast transformation to β-TCP[2]. XRD and Rietveld refinement were employed to determine the phase composition after the thermal treatment.

Table 1. Parameters of α-TCP cylinders prior to calcination at 900 °C.

Sample	LPR [g/g]	Porosity [%]
Porous	0.70	45 (2)
Medium	0.55	43 (2)
Dense	0.40	36 (1)
Dense + PAA	0.325	32 (1)

RESULTS: Figure 1 shows the gradual transformation of α-TCP to β-TCP at 900 °C, and a quite obvious dependency between transformation rate and the amount of porosity. The sample containing PAA was denser and transformed faster than PAA-free samples, but since PAA introduced trace amounts of Na^+, the results may not be directly comparable. With the exception of sample "Dense + PAA", the degradation of α-TCP is accurately described by the Avrami[3] equation with a correlation coefficient $r^2 > 0.995$:

$$Y = A \cdot exp(-K \cdot t^n) \qquad (1)$$

A being the α-TCP content at time 0, *t* the calcination time, and *K* and *n* being constants.

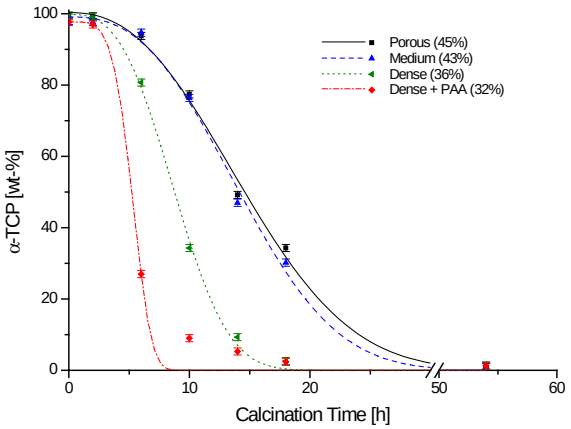

Fig. 1: Evolution of α-TCP content as a function of porosity and calcination time at 900 °C.

Table 2. Fitted constants K and n from eq. (1) of the 3 PAA-free samples (std. err. in parentheses).

Sample	*K*	*n*
Porous	0.0011 (0.0008)	2.4 (0.3)
Medium	0.0007 (0.0006)	2.6 (0.3)
Dense	0.0013 (0.0007)	2.9 (0.2)

DISCUSSION & CONCLUSIONS: The existence of a correlation between transformation rate of α-TCP to β-TCP and porosity of the bulk sample was demonstrated. Experiments at temperatures below and above 900 °C should provide more detailed information on the driving mechanisms behind the transformation, e.g. on the temperature dependency of nucleation and grain growth. This will be investigated in more detail later in this project.

REFERENCES: [1] J.H. Welch, W. Gutt (1961) *J Chem Soc* **874**:4442-4. [2] H. Monma, M. Goto (1983) *Yogyo-Kyokai-Shi* **91[10]**:473-5. [3] M. Avrami (1939) *J Chem Phys* **7[12]**:1103-12.

Osteogenic differentiation of human bone marrow stromal cells via polycaprolactone roughness gradients in the absence of dexamethasone

A.B. Faia-Torres[1,3,4], M. Rottmar[2], S. Lischer[2], T. Goren[1], M. Charley[1], K. Maniura-Weber[2], N.D. Spencer[1], M. Textor[1], R.L. Reis[3,4], N.M. Neves[3,4]

[1] Laboratory for Surface Science and Technology, ETH Zurich, CH. [2] Laboratory for Materials-Biology Interactions, Empa, Swiss Federal Laboratories for Materials Testing and Research, CH. [3] 3B's Research Group – Biomaterials, Biodegradables and Biomimetics, University of Minho, Portugal. [4] IVCS/3B's – PT Government Associate Laboratory, Portugal

INTRODUCTION: Tissue engineering is expected to enable the development of new therapies for bone regeneration. Surface characteristics of the cellular support influence tissue healing and, therefore, the success of the implant. We studied the cellular amplification and the osteogenic differentiation potential of human bone marrow stromal cells (hBMSC) seeded on a micro- to nanoscale roughness gradient imprinted in polycaprolactone (PCL) membranes. PCL is an FDA-approved biocompatible and biodegradable polymer. By using cells with high proliferative potential and culturing them in those substrates we aim at providing a niche stimulating the synthesis of bone matrix. Using this platform, we tested in a very tightly controlled environment, the effect of the roughness that elicits strong adhesion and proliferation of hBMSCs. Furthermore we also evaluate the effect of roughness over the course of the osteogenic differentiation in the absence of the osteoinductive supplementing agent dexamethasone, which is required to obtain successful osteogenic differentiation.

METHODS: Aluminium gradient masters (sand blasted and then chemically polished) were cast into polyvinylsiloxane and transferred to epoxy.[1,2] The epoxy replicas were then used as masters, and hot-embossed into a solvent-cast membrane of PCL at 70ºC for 10 minutes. After curing, the newly created polymeric gradients were sterilized by plasma treatment, resulting in a roughness gradient varying in average amplitude (R_a) from 4.9µm to 21nm. PCL gradients were cultured with hBMSCs at passage 1, under three culture conditions: stemness maintenance medium (control), osteogenic differentiation medium with dexamethasone (positive control) and osteogenic differentiation medium without dexamethasone.

RESULTS: As expected, HBMSCs cultured in maintenance medium, along the time period of 14 days, showed no expression of alkaline phosphatase (ALP), an earlier marker of osteogenesis. In contrast, normalized ALP expression per number of cells per square millimeter suggests that when cultured in medium without dexamethasone, a cell population above 400 counts per square millimeter is able to express ALP differentiation marker even in less favourable conditions (i.e., areas with nanoscale roughness). The differentiation occurs faster (since day 7, *Figure 1*) and more consistently (for all time points) in areas with microscale roughness. In medium supplemented with dexamethasone, the ALP expression is consistently most supported in regions having roughness in the nanometer range.

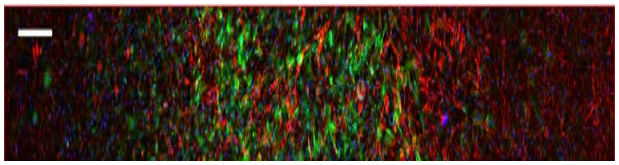

Fig. 1: ALP expression along the roughness gradient (from nano- to microscale roughness, from left to right) in differentiation medium without dexamethasone, at the 7th day of culture, captured by fluorescent microscopy. The scale bar corresponds to 500 microns. ALP is shown in red, actin in green and nuclei in blue.

DISCUSSION & CONCLUSIONS: We demonstrate that in the absence of the strong chemical inducer of osteogenic differentiation, dexamethasone, specific surface roughness encourages human BMSC towards the osteoblastic lineage. Our results also lead to further understanding about the influence of adhered cell numbers on the osteogenic differentiation of hBMSCs cultured on rough surfaces. This strategy enables obtaining new insights into the use of specific roughness ranges that will facilitate successful bone healing.

REFERENCES: [1] M. Wieland, B. Chehroudi, M. Textor, et al (2002) *J Biomed Mater Res*, **60**:434-44. [2] M. Schuler, T. P. Kunzler, M. de Wild, et al (2009) *J Biomed Mater Res*, **88A**:12-22.

Nanoencapsulation of silver-based drugs

J. Gagnon[1], K.M. Fromm[1]

[1]*Fromm Group, Department of Chemistry, University of Fribourg, Fribourg, CH.*

INTRODUCTION: Silver compounds and silver nanoparticles are gaining more and more interest from the scientific society as a replacement to antibiotics. However, these compounds may be too soluble and even toxic for the host. Encapsulation might be very advantageous in order to increase the stability and biocompatibility of silver drugs. In this research, cerium oxide, also called ceria, nanocapsules were synthesized due to the high stability and low toxicity of this material.[1] CeO_2 capsules were then used to encapsulate the silver compound $Ag(L)NO_3$ illustrated in Figure 1.

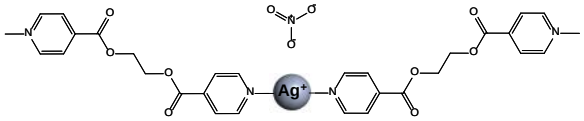

Fig. 1: Representation of an excerpt of $Ag(L)NO_3$.

METHODS: CeO_2 nanocapsules were synthesized first by making anionic polystyrene spheres, followed by the coating of these spheres with ceria, and the removal of the core by calcination.[2]

The silver-containing compound $Ag(L)NO_3$ was encapsulated in two steps: by inserting first silver nitrate and then the ligand in such a way that the complexation can occur inside the capsules. To do so, at each step, the capsules were submitted to vacuum, immersed in saturated solution of the desired compound and then washed a few times.

RESULTS: The synthesized nanocapsules were composed of cerium oxide, as determined by powder XRD (not shown). From the TEM images (Figure 2) and from the disappearance of the polystyrene bands on the IR spectra (not shown), it is demonstrated that the core was completely removed after calcination resulting in empty capsules. Figure 3 shows the TGA of the capsules loaded with $Ag(L)NO_3$. The degradation of $Ag(L)NO_3$ is retarded to 320°C when it is encapsulated compared to the free $Ag(L)NO_3$ which degrades at 210°C.

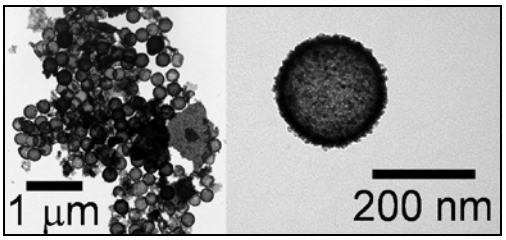

Fig. 2: TEM images of empty ceria nanocapsules.

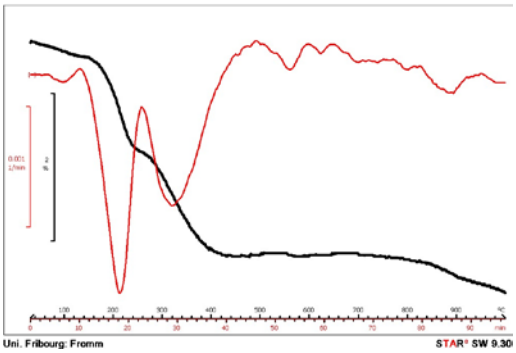

Fig. 3: TGA of $Ag(L)NO_3$ encapsulated in CeO_2 capsules (black) and its derivative (red).

Silver release experiments were also performed using ICP-OES (not shown) and demonstrate that $Ag(L)NO_3$ encapsulated in CeO_2 capsules can release silver over a period of at least one week.

DISCUSSION & CONCLUSIONS: Ceria nanocapsules were successfully synthesized. TGA and release experiments give promising results for the encapsulation of antimicrobial silver compounds. More experiments and analysis will be performed to study the encapsulation of silver nanoparticles and complexes as well as their respective silver release. The antimicrobial efficiency of these systems will also be analyzed. Finally, the biocompatibility in terms of cellular adhesion and toxicity will be studied in order to allow the implantation into patients.

REFERENCES: [1] T. Xia, et al (2008) *Nano* **2**:2121-2134. [2] I.A. Kartsonakis, et al (2008) *J Am Ceram Soc* **91**:372-378

ACKNOWLEDGEMENTS: We are grateful to the Swiss National Science Foundation, the University of Fribourg and FriMat for generously supporting this project.

Synthesis and antibacterial activity of nanohydroxyapatite/ZnO nanoparticles composites

L Grenho[1,2], FJ Monteiro[1,2], MP Ferraz[1,3]

[1] INEB - Instituto de Engenharia Biomédica, Universidade do Porto, Porto, Portugal. [2] DEMM, Faculdade de Engenharia, Universidade do Porto, Porto, Portugal. [3] CEBIMED - Centro de Estudos em Biomedicina, Universidade Fernando Pessoa, Porto, Portugal

INTRODUCTION: In orthopedics due to the enormous number of surgical procedures involving invasive implant biomaterials, infections have a huge impact in terms of morbidity, mortality, and medical costs [l]. This has been the driving force for the development of new surfaces with antibacterial agents that might affect differently several microorganisms, together with the fact that the biomaterial must possess good biocompatibility, be bioactive and show good osseointegration capability. In the present work, nanohydroxyapatite (nanoHA), a material used for bone regeneration applications [2], was combined with nanoparticulated zinc oxide (ZnO), which is known to have antibacterial activity [3]. NanoHA/ZnO composite was characterized by SEM-EDX and antibacterial studies were performed.

METHODS: ZnO nanoparticles (~100nm diameter; Sigma-Aldrich) were added to nanoHA powder (nanoXIM·HAp202; Fluidinova S.A., Portugal) at weight percentages of 0%, 2% and 10%. The powders were stirred for 12h and then uniaxially pressed (Mestra Snow, P3) to cylindrical samples with 10mm diameter. The composites morphology and elemental composition were characterized by scanning electron microscopy (SEM) and energy-dispersive X-ray spectroscopy (EDX), respectively. The antibacterial activity was performed with Gram positive bacteria *S. aureus* ATCC 25923. The disc shaped samples were seeded with a bacterial concentration of $1{,}5\times10^8$/ml, in tryptic soy broth (TSB). After 24h of incubation at 37°C, adherent cells number was quantified as colony forming units (CFU) after being released by sonication.

RESULTS: Surface morphology of the composites as viewed by SEM revealed the presence of ZnO nanoparticles at the nanoHA surface (Fig. 1) and EDX analysis confirmed that presence in both nanoHA composites. CFU data indicated that, while for the composite with low of ZnO nanoparticles weight ratio (2 wt %) slightly reduced the density of bacteria, for higher weight ratio (10 wt %) the reduction in bacterial adhesion was much more significant than both for low weight ratio composite and pure nanoHA samples.

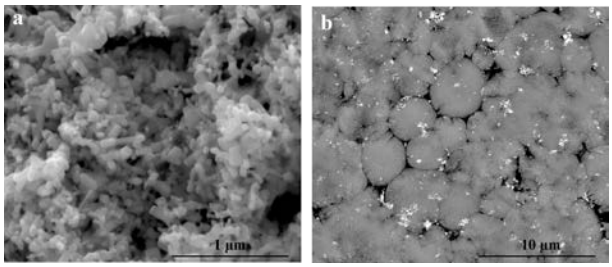

Fig. 1: SEM images of ZnO nanoparticles (a) and nanoHA-10 wt % ZnO composite (b).

DISCUSSION & CONCLUSIONS: In this study, nanoHA/ZnO nanoparticle composites were successfully prepared and antibacterial activity was observed when these composites were tested against Gram positive *S. aureus*. The results found in this work indicated that nanoHA/ZnO composites shows significant antibacterial activity in the presence of 10 wt % ZnO, as considerable reduction in the number of bacteria over the samples' surfaces was observed. This suggests that the nanoHA/ZnO composites could be considered for biomaterial applications prone to excessive bacterial growth, such as orthopaedic implants, due to their ability to reduce bacterial adhesion/activity and consequent biofilm formation.

REFERENCES: [1] Cataldo, et al (2010) *J Infect* **61**:443-8. [2] Ferraz, et al (2004) *J Appl Biomater Biomech* **2**:74-80. [3] Raghupathi, et al (2011) *Langmuir* **27**:4020-8.

ACKNOWLEDGEMENTS: This work was financed by FEDER (COMPETE) and by FCT in the framework of the NaNOBiofilm project (PTDC/SAU-BMA/111233/2009) and PhD grant (SFRH/BD/72866/2010), whose support is acknowledged.

Human progenitor tenocytes for re-cellularization of matrix for rotator cuff repair

A Grognuz[1], A Farron[2], W Raffoul[1], LA Applegate[1]

[1]*Unit of Regenerative Therapy, Service of Plastic and Reconstructive Surgery, and* [2]*Service of Orthopedics, Centre Hospitalier Universitaire Vaudois, Lausanne, CH*

INTRODUCTION: Tendon rupture within the shoulder can be a serious problem with the rotator cuff tendon being one of the most common injured tendons of the body. Surgical intervention can use biomaterials for repair of defects. Matrix associated with specific cells can provide a tissue engineering solution ideal for rotator cuff repair. Cell choice has to be adaptable to clinical practice (GMP processing) and to show high cell proliferation, adhesion and biocompatibility to matrix products available. Human progenitor tenocytes provide an interesting cell source for re-seeding matrix that have biomechanical support necessary and possess biocompatibility towards matrix materials available.

METHODS: Cell metabolism of human tenocyte progenitor cells (FE002-Ten.R, established in our lab) was tested between passages 3 to 9 with a Cell Titer Assay (absorbance 492 nm). Cells are grown in DMEM + 10% FBS and evaluated every 3-4 days up to day 25. Molecules for characterization were assessed by flow cytometry (CD14, CD90, CD166, CD44, CD105, CD34, CD19, CD73 and immunogenic epitope HLA-DR, DP, DQ). Cells were also grown at high density in 3D pellets to control their viability and assess functional activity by matrix deposition. Pellets were grown for 14 days, embedded in paraffin, sectioned at 4µm and stained to evaluate the morphology and function of micro-tissues.

RESULTS: Cell growth portrayed that more than 40 percent of metabolism is maintained even at late passages compared to early passage cells (between passage 3 and up to passage 9).

Flow cytometry analysis shows that 99% of the gated cells are alive and that there is a unique cell type in the population with uni-modal distribution. HLA-DR, DP, DQ is not expressed. Surface markers CD90, CD166, CD105 and CD 73 are positive while CD14, CD44, CD34 and CD19 are negative.

Histological sections of cells grown for 14 days in high density pellets show uniform cellular matrix deposition as illustrated in Figure 1.

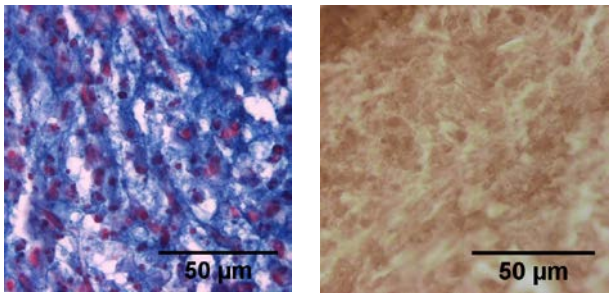

Figure 1 : Alcian blue staining showing the production of sulfated glycosaminoglycans in pellet (left). Type-1 collagen within pellet (right, DAB immunostaining).

DISCUSSION & CONCLUSIONS: The human progenitor tenocytes evaluated in this study maintain a high metabolism even in passages far beyond those usually employed for clinical applications, thus they may be an optimal cell choice due to their stability. Expression of HLA-DR, DP, DQ is not observed, which assures a potential cell source for transplantation. Moreover, their ability to live in high density three-dimensional pellet formats and to produce matrix is a positive attribute. Other human progenitor cells have been used successfully in the clinic for treatment of wounds and burns [1; 2]. Overall, human progenitor tenocytes may be an interesting cell source in the aim to improve rotator cuff injury repair.

REFERENCES: [1]AS De Buys Roessingh, J. Hohlfeld, C. Scaletta et al (2006) *Cell transplant* **15**: 823-34. [2]J. Hohlfeld, A. de Buys Roessingh, N. Hirt-Burri et al (2005) *Lancet* **366**: 840-2.

ACKNOWLEDGEMENTS: These studies were funded by the Inter-institutional Center for Translational Biomechanics EPFL/CHUV/DAL and by the Foundations S.A.N.T.E and Sandoz family.

Towards optimized fluoride particles for dental care applications

Joachim Köser and Uwe Pieles

School of Life Sciences, University of Applied Sciences and Arts Northwestern Switzerland, Muttenz, Switzerland.

INTRODUCTION: The use of fluoride containing dental care products has a beneficial effect on the reduction of caries progression[1]. On the enamel surface of teeth treated with soluble fluoride ions calcium fluoride particles are formed which serve as a reservoir for fluoride in the time interval between the applications[2]. Little is known about the formation of these particles as well as their adhesion to the tooth enamel and their dissolution over time, especially during cariogenic challenges. The aim of the project presented here is to get more insights into the CaF_2 particle formation process and to optimize these particles with respect to adhesion and fluoride release kinetics.

METHODS: CaF_2 particles were synthesized by mixing of precursor solutions with soluble calcium and fluoride salts in different ratios. Following their assembly the particles were purified by centrifugation and washed in saturated CaF_2 solution. Analysis of the particle morphology was performed by scanning electron microscopy.

RESULTS: Calcium fluoride particles described in the literature are reported to exhibit either cubic, when formed in situ, or more globular shapes, when assembled on the surface of tooth enamel. We were able to generate in situ CaF_2 particles resembling both morphologies by tuning the mixing ratio of soluble calcium and fluoride ions. Particles ranging from approximately 50 nm to several µm diameter could be produced. Their shapes range from perfectly cubic to more octahedral and round (examples see Fig. 1 and 2).

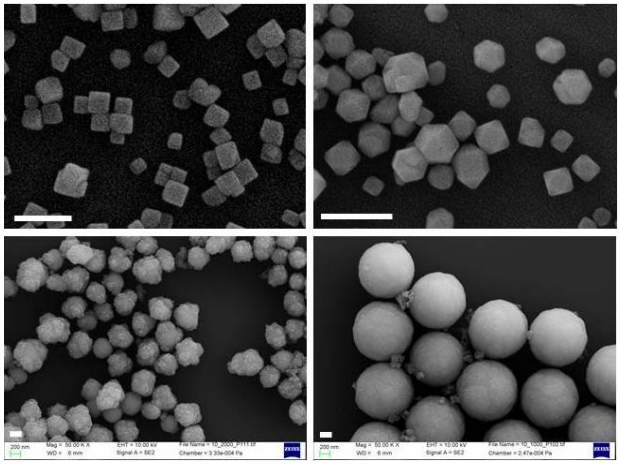

Fig. 1: SEM gallery of CaF_2 particles obtained by variation of the parent salt concentrations. NaF and $CaCl_2$ salt solution were mixed and the resulting particles purified and analysed by scanning electron microscopy. The white scale bars represent 200 nm.

In certain instances continuous transitions between different shapes can be obtained. One example is shown in Fig 2, where by varying the concentration of one of the parent salt solutions a change from round to cubic CaF_2 particles can be observed.

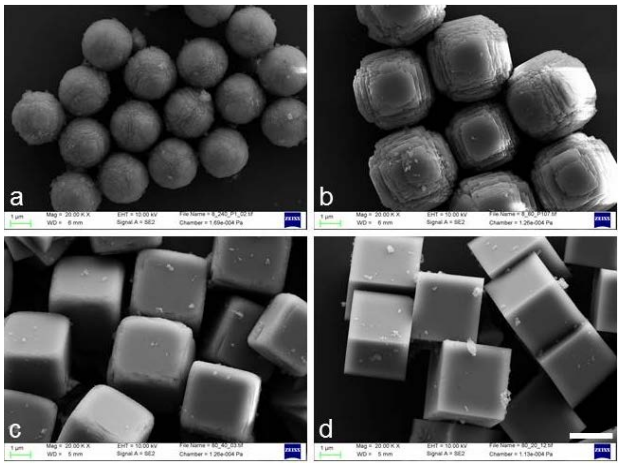

Fig. 2: Continuous transition of the shape of CaF_2 particles by varying the concentration of Ca^{2+} during assembly (a-d). The white scale bar represents 2 µm.

DISCUSSION & CONCLUSIONS: Here we demonstrate the generation of polymorphic CaF_2 particles by variation of the concentrations of the comprising Ca^{2+} and F^- ions. As a general tendency lower concentrations of the parental ions result in larger particle sizes, whereas round and cubic assembly shapes can be observed at different mixing ratios independent of the absolute amount of either Ca^{2+}, F^- or a fixed stoichiometry. In a next step the different CaF_2 particles will be analyzed with respect to adhesion on enamel surfaces and their fluoride release kinetics.

REFERENCES: [1] Mani (2009) *Arch Orofacial Sci* **4**:1-6; [2] Petzold (2001) *Caries Res* **35(suppl 1)**: 45–51.

ACKNOWLEDGEMENT: The authors acknowledge the financial support by the Swiss

Nanoscience Institute and the help from the members of the Nanotechnology and Materials Sciences group of the FHNW.

Nitroxide Antioxidants Immobilized on the Metal Oxide Surface

J. Kurz[1], A. Leisibach[1], U. Pieles[1], M. de Wild[1]

[1] *University of Applied Sciences Northwestern Switzerland, Muttenz, Switzerland*

INTRODUCTION: Biocompatible biomaterials are becoming more and more important in the practice of modern medicine. Unfortunately, almost all implantable devices suffer, to a different extent, from adverse reactions, including fibrosis, thrombosis, inflammation and/or infection [1]. To reduce the failure rates and to improve the implant function higher quality biomaterials must be developed [2]. Immobilization of nitroxide molecules on the surface of biomaterial offers an attractive, direct and interactive approach to regulate the redox homeostasis of the surrounding cells and ensures the local activity of antioxidant against ROS (reactive oxygen species), what enhances the therapeutic effect *in situ* and minimizes the potential systemic toxicity. The multimode way of nitroxide action and the diversity of mechanisms underlying their activity may lead to a new, simple therapy that would bring together most of hitherto studied approaches [3,4].

METHODS: Nitroxide molecules were covalently immobilized to a metallic implant material either directly or via a linker molecule, as shown in Fig. 1.

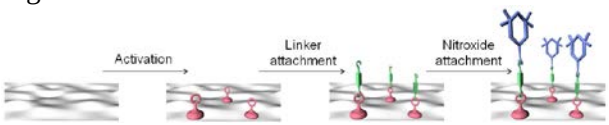

Fig. 1: A graphical illustration of nitroxide attachment to the metal oxide surface.

In a straightforward functionalization strategy, nitroxide molecules, previously coupled to silane linker, were directly attached to the metal oxide surface.
In a two-step attachment process, the reaction between the hydroxyl-terminated surface and silane linker was followed by the reaction of functional silane group with the nitroxide molecule. Several approaches have been explored using various trialkoxysilanes, e.g. glycidoxy-propyltriethoxysilane (GOPS) and aminopropyl-triethoxysilane (APTES). These types of silanes tend to polymerize and form a thick-film layer, thus they should help to increase the concentration of nitroxides linked to the surface.

XPS and low temperature EPR methods were used to verify the successful coating strategies.

RESULTS: The successful introduction of the nitroxide functionality was confirmed by the presence of N 1s signal in the XPS spectra (Fig. 2).

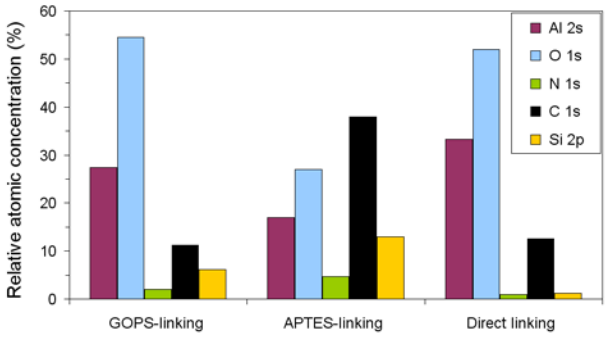

Fig. 2: Sample XPS data for aluminium oxide surface modified with nitroxide compounds.

Since, in case of nitrogen-containing APTES silane, the presence of N 1s signal is not conclusive evidence for the presence of nitroxides, the EPR spectra at 100K were additionally registered (data not shown). Quantification of the XPS spectra provides information about the stoichiometry of the linkage chemistry. In the direct immobilization process, nitroxide-silane adduct seems to show lower reactivity towards the surface and lower ability to create thick multilayers.

DISCUSSION & CONCLUSIONS: We have investigated methods to functionalize metal oxide surfaces by an anti-oxidative/anti-inflammatory coating using nitroxide compounds.
Detailed *in vitro* investigations of nitroxide-coating activity against ROS remain a challenge which we continue to tackle, to demonstrate the great potential of nitroxides, already proven in many other cases [4].

REFERENCES: [1] K.S. Jones (2008) *Seminars in Immunology* **20**:130-36. [2] H. Park, et al (2006) *Am J Orthod Dentofacial Orthop* **130**:18-25. [3] P.M. Mountziaris, et al (2008) *Tissue Engineering B* **14**:179-86. [4] S. Cuzzocrea, et al. (2001) *Pharmacol Rev* **53**:135-59.

ACKNOWLEDGEMENTS: The project team gratefully acknowledges the financial support of the strategic funding program of the School of Life Sciences, University of Applied Sciences Northwestern Switzerland.

Different cell fate for human osteoblasts and osteosarcoma cell line MG63 on implant surfaces

S.Lischer[1], M.Rottmar[1], U.Tobler[1] K.Maniura-Weber[1]

[1] *Empa, Swiss Federal Laboratories for Materials Science and Technology, Lerchenfeldstr. 5, CH-9014 St. Gallen*

INTRODUCTION: Osteosarcoma cell lines like MG63, Saos-2 or U-2 OS are commonly used as osteoblastic in vitro models to investigate cellular behaviour on implant materials[1]. Osteosarcoma cells originate from malignant bone tumors. They have an aneuploid chromosome pattern, tend to proliferate rapidly and show an unlimited life span which delivers a phenotypically stable cell population, but the chromosomal alteration lead to abnormal cellular functions[1]. Primary osteoblasts in contrast have a diploid chromosome pattern and are characterized by slow cell proliferation with a finite life span[2]. Cell adhesion is a complex process that is crucial for implant integration. For adherent cells the initial cell attachment to the material surface is important for subsequent cell fate like cell growth, proliferation or differentiation[2]. Primary osteoblasts are anchorage dependent cells, if they cannot adhere and spread on the surface they lose their viability. Our aim was therefore to study differences in cell behaviour of cell lines and primary cells upon cultivation on implant surfaces.

METHODS: Human primary bone cells (HBC) or MG63 osteosarcoma cells were seeded onto implant surfaces and cultivated in either osteo-specific proliferation or differentiation media. Cellular response was determined by analysis of proliferation via DNA assay. The differentiation potential of the cells were analysed by immuno-histochemical staining for bone proteins ALP and Col-I as well as gene expression analysis by qRT-PCR.

RESULTS: The identical cell density of MG63 and HBC was applied to materials to determine the amount of DNA at various time points. MG63 cells showed a higher amount of DNA on tissue culture petri dishes compared to primary human osteoblasts over a period of seven days.

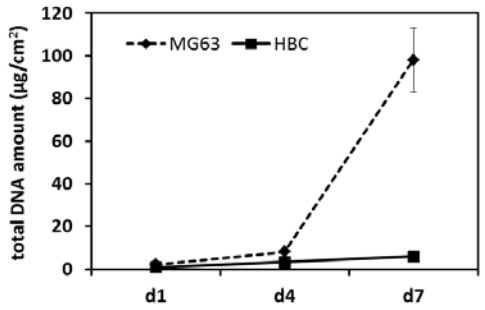

Fig 1: Determination of DNA amount of MG63 and HBC on TCP.

Primary human osteoblasts showed a higher differentiation potential as indicated by amounts of osteocalcin and ALP mRNA as well as mineralisation whereas MG63 cells showed a low ALP mRNA level and no mineralisation potential. Further, for both cell types it was shown that ALP and OC gene expression is dependent on cell density.

DISCUSSION & CONCLUSIONS: This work demonstrated that cell lines and primary cells show different cell behaviour on materials. MG63 cells attached faster to the investigated implant surfaces and showed therefore also a better cell proliferation on the materials than primary osteoblasts. The advantage of using primary osteoblasts is their superior differentiation potential and the diploid chromosome pattern which provides a better model for the in vivo simulation. Primary osteoblasts appear to be more sensitive to implant surfaces and for that reason more relevant for in vitro tests.

REFERENCES:

[1]C. Pautke et al. (2004) *Anticancer Res* **24**:3743-3748. [2]A.L. Pérez et al (2003) *Int Endodontic J*, **36**.

Engineering MSC condensations for cartilage tissue engineering

Christopher Millan[1], Yuan Yang[2], Thomas Groth[2], Janos Vörös[3], Marcy Zenobi-Wong[1]

[1] *Cartilage Engnieering and Regeneration Lab, ETH Zürich, Zürich, CH.*

[2] *Biomedical Materials Group, Martin Luther University Halle-Wittenberg, DE*

[3] *Laboratory for Biosensors and Bioelectronics, ETH Zürich, Zürich, CH*

INTRODUCTION: Engineering cartilage which can meet the functional demands placed on the tissue in-vivo has yet to be realized and addresses an important clinical need. We have focused on establishing a system that mimics the early stages of skeletal morphogenesis during which mesenchymal stromal cells (MSCs) condense prior to differentiation into chondrocytes, a necessary step that triggers chondrogenic differentiation. We are currently exploring a technique whereby stem cells are coated with polyelectrolyte nanofilms in a layer-by-layer (LbL) fashion. These nanofilms have shown promise for augmenting cell-cell interactions promoting high density culture conditions by way of specific and electrostatic interactions depending on the nature of the layering molecules. Furthermore, co-cultures can be made with MSCs and mature chondrocytes where signalling between the two cell types may help in phenotypic stabilization.

METHODS: Formation of nanofilms around cells was performed using an LbL technique. Cells were initially incubated for 15 minutes in a solution of 0.06 mg/mL fibronectin (PBS, pH 6.5). Subsequent solutions of increasingly concentrated gelatin (G) or fibronectin (Fn) were added to the cell suspension where the excess concentration species was deposited as a layer in the nanofilm on the cell surface desired thickness was reached. These experiments were also performed with poly-L-lysine (PLL) and oxidized chondroitin sulphate (oxCS). Quart crystal microbalance with dissipation (QCM-D) measurements were used to follow LbL buildup where layering solutions were prepared by a 1:1 dilution of the excess concentration species with the solution used for the previous layer. MSCs and bovine chondrocytes (bCh) were labelled with fluorescent tracer molecules, coated with Fn-G or PLL-oxCS nanofilms, and seeded at high density for rapid tissue assembly. Constructs were observed with confocal microscopy (CLSM) and assessed for degree of cell-cell interaction.

RESULTS: QCM-D measurements show clear LbL build-up of nanofilms. Compared with traditional methods of producing PEMs, the titration technique using heterogeneous solutions resulted in nanofilms exhibiting over 5x greater shifts in quartz crystal resonance frequency. Cell viability was not significantly affected by coating with titration, whereas including washing and centrifugation steps resulted in loss of over 50% of the initial cell population. Chondrocytes and stem cells coated with nanofilms (Fig 1b) exhibited enhanced interactions between adjacent cells and resulted in both an increased size of the cell agglomerations and cell packing density as well as reduced space between agglomerations versus uncoated controls (Fig 1d).

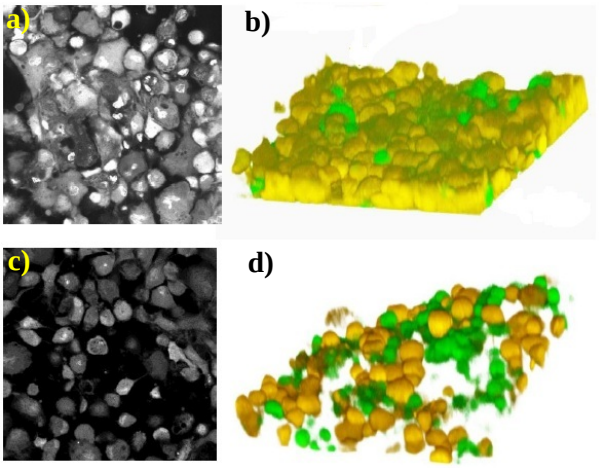

Fig. 1: CLSM cross sections (a and c) and 3D reconstructions (b and d) of MSC (orange) and bCh (grn) co-cultures. Cells coated with nanofilms of Fn-G (a and b) exhibited higher cell densities in microtissue constructs than uncoated controls (c and d).

DISCUSSION & CONCLUSIONS: A novel system for coating and co-culturing heterogeneous cells is introduced. It offers great versatility for monitoring the interactions of the two cell types in-situ and may also prove useful as an engineered construct in cartilage defect repairs.

ACKNOWLEDGEMENTS: This work is supported by the Swiss National Science Foundation (CR23I2-130678/1) and FP7 "Find & Bind" (NMP4SL2009229292).

MWCNT reinforced PLLA composite - a good candidate to produce bone implants?

M. Obarzanek-Fojt[1], E. Lizundia[2], JR. Sarasua[2], A. Bruinink[1]

[1]*Materials-Biology Interactions, EMPA, St. Gallen. Switzerland.* [2]*Department of Mining-Metallurgy and Materials Science, University of the Basque Country (EHU-UPV), 48013 Bilbao*

INTRODUCTION: Since their discovery in 90-ties last century, the multiwall carbon nanotubes (MWCNT) found many applications in different fields. Thanks to their excellent mechanical properties MWCNT are lately of special interest in the preparation of reinforced biodegradable composites with specific biomedical applications where resistant but still bio-resorbable materials are indispensable. Even though some groups reported already the effect of MWCNT on cellular metabolism in different systems, still remains unclear whether MWCNT could have some beneficial role on bone cells. Recently it has been reported by the others that poly(l-lactide) (PLLA):MWCNT composite inhibits fibroblast proliferation *in vitro* [1]. Here we demonstrate in more details the effect of PLLA:MWCNT composite on cell adhesion, proliferation and differentiation with a specific respect to bone cells.

METHODS: The multiwall carbon nanotubes (MWCNT) were synthesized by Arkema in Catalytic Chemical Vapor Deposition (CCVD) process. Poly(L-lactide) from Purac Biochem (NL) was used as matrix to prepare nanocomposites. Effect of MWCNT or PLLA:MWCNT composite on cell toxicity was evaluated either with 3T3 fibroblast cell line or with primary human bone marrow stromal cells (HBMC). In order to test cell potential to colonize the PLLA:MWCNT composite three dimensional cell spheroids were generated. The effect of PLLA:MWCNT composite surfaces was further evaluated on HBMC cell differentiation towards osteogenesis via quantitative RT-PCR or FACS analysis for the expression of bone specific genes.

RESULTS: Our data indicate that suspended MWCNT have no adverse effect on proliferation and activity of bone marrow stromal cells within tested nanotubes concentration range. We did not observe any toxic response on 3T3 fibroblast cell line cultured in the presence of eluent prepared form PLLA:MWCNT composites. Moreover human bone marrow stromal cells can easily attach to the surface of PLLA composite containing different concentration of MWCNTs. Bone marrow stromal cells spheroids adhered to the composite surface and cell outgrowth from three-dimensional cell reaggregates was observed. There was no adverse effect on bone marrow stromal cell differentiation towards osteoblast when HBMCs were cultured on composite surfaces.

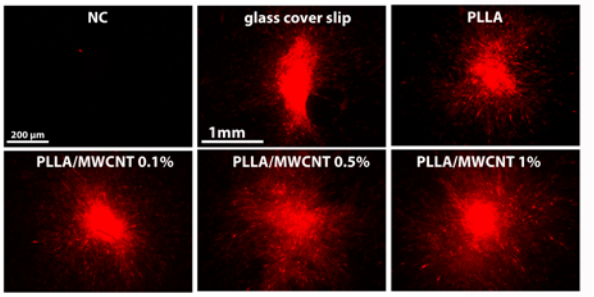

Fig. 1: Cell outgrowth from three dimensional spheroids composed exclusively of human bone marrow stromal cells on PLLA:MWCNT composites containing different concentration of multiwall carbon nanotubes.

DISCUSSION & CONCLUSIONS: Our data indicate that the MWCNTs have no adverse effect on the metabolism of bone marrow stromal cells. When cultured under the osteogenic condition and in the presence of MWCNTs the bone marrow stromal cells undergo differentiation toward pre-osteoblast state as efficient as not treated control cells. Moreover, PLLA:MWCNT composite supported colonization and differentiation of human bone marrow stromal cells. Presented data indicate that MWCNT may be used to reinforce the biodegradable composites without inducing toxic response in bone cells and as such are good candidate in the biomedical application.

REFERENCES: [1] D. Zhang et al (2006) *J Phys Chem B* **110**(26):12910-12915.

ACKNOWLEDGEMENTS: This work has been supported by EC FP7 POCO, Grant agreement number: CP-IP 213939-1

Evaluation of a thermoresponsive hyaluronan hydrogel as stem cell carrier for intervertebral disc regeneration

M Peroglio[1], D Eglin[1], LM Benneker[2], M Alini[1], S Grad[1]

[1]*AO Research Institute Davos, Davos, CH.* [2]*University Hospital Bern, Bern, CH.*

INTRODUCTION: Mesenchymal stem cells (MSCs) have shown potential for intervertebral disc (IVD) regeneration. However, MSC survival and differentiation is strongly affected by the IVD environment, which is hypoxic and displays low glucose concentration and pH. A potential technique to improve MSC fate in the IVD is MSC pre-differentiation with appropriate carriers and growth factors (GF) [1]. Thermoresponsive hydrogels are advantageous as cells can be collected after pre-culture by cooling and then injected in the IVD [2,3]. The aims of this study were to investigate (i) whether a thermoresponsive hyaluronan-based hydrogel could support MSC differentiation toward the nucleus pulposus (NP) phenotype and (ii) whether the supplementation of GF could further improve MSC differentiation.

METHODS: Hydrogel preparation: Thermoresponsive polymers were prepared from hyaluronic acid (HA) (Sigma-Aldrich) and poly(N-isopropylacrylamide) (pNIPAM) (M_n=20x10^3 g·mol^{-1}) as previously described [2,3]. Hydrogels were obtained by mixing HA-pNIPAM in phosphate buffered saline (12% wt/vol). **In vitro differentiation of MSCs:** Human bone-marrow derived mesenchymal stem cells (hMSCs) were suspended in either HA-pNIPAM solution or 1.2% alginate (8x10^6 cells/mL). Gel beads were formed by dropping the cell suspension in the medium at 37°C or by cross-linking alginate in a 100 mM $CaCl_2$ solution. Beads were cultured for one week under hypoxic conditions (5% O_2) in chondropermissive medium (DMEM 4.5 g/L glucose, 1% non-essential amino acids, 1% insulin-transferrin selenium premix, 50 µg/mL ascorbate-2-phosphate and 10^{-7} M dexamethasone) with or without the addition of growth factors (100 ng/mL of growth and differentiation factor 5 (GDF5) or 10 ng/mL of transforming growth factor β1 (TGF-β1)). Samples were quantified for DNA (by Picogreen) and glycosaminoglycan (GAG) (by dimethylmethylene blue); real-time PCR was performed using relevant markers for disc-like differentiation.

RESULTS: DNA was slightly higher in MSC-seeded alginate compared to HA-pNIPAM, while GAG followed an opposite trend. As an outcome, GAG/DNA was higher in HA-pNIPAM than alginate, especially with the addition of GF. On the mRNA level, HA-pNIPAM supported hMSC differentiation toward the NP phenotype compared to alginate, even without the supplementation of GF (fig.1). In HA-pNIPAM cultures, the addition of GDF5 and TGF-β1 similarly improved the COL2/COL1 ratio, while in alginate cultures TGF-β1 had a much stronger effect than GDF-5.

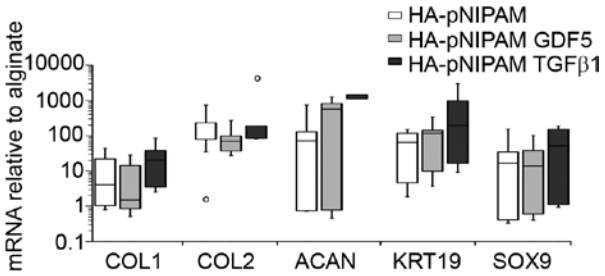

Fig. 1: Gene expression profile of hMSCs after one week of culture in HA-pNIPAM under hypoxia and in chondropermissive medium with or without GF. Data are represented relative to hMSCs cultured in alginate in chondropermissive medium without GF supplementation, ° are outliers.

DISCUSSION & CONCLUSIONS: Based on the GAG/DNA and gene expression profile of hMSCs (fig.1), HA-pNIPAM seems a more adequate carrier than alginate for in vitro hMSC differentiation toward the NP phenotype. The different hMSC response to GF in HA-pNIPAM compared to alginate is likely due to strong effect of HA itself and differences in the diffusion properties of the two materials. In conclusion, culture in HA-pNIPAM hydrogel is sufficient for MSC disc-like differentiation without the need of GF supplementation.

REFERENCES: [1]B. Gantenbein-Ritter, L.M. Benneker, M. Alini, et al (2011) *Eur Spine J* **20**:177-86. [2]D. Mortisen, M. Peroglio, M. Alini, et al (2010) *Biomacromol* **11**:1261-72. [3]M. Peroglio, S. Grad, D. Mortisen, et al *Eur Spine J* (Epub ahead of print).

ACKNOWLEDGEMENTS: This study was partially supported by a NASS Research Grant.

Influence of surface proteins on *Staphylococcus epidermidis* adhesion to nanohydroxyapatite as a substrate for bone regeneration

M Ribeiro[1,2*], L Grenho[1,2*], FJ Monteiro[1,2], MP Ferraz[1,3]

[1] *INEB - Instituto de Engenharia Biomédica, Universidade do Porto, Porto, Portugal.* [2] *Universidade do Porto - Faculdade de Engenharia, DEMM, Porto, Portugal.* [3] *CEBIMED - Centro de Estudos em Biomedicina, Universidade Fernando Pessoa, Porto, Portugal.* [*] *Contributed equally*

INTRODUCTION: *Staphylococcus epidermidis* has been frequently associated with infections involving materials for orthopaedic applications due to its abilities to adhere to surfaces and to form biofilms, which are resistant to antibiotic therapy and host cell-mediated defenses [1]. Moreover, one important factor, which has been calling attention regarding biomaterials, is how the material surface characteristics will be affected by the deposition of proteins when in "*in vivo*" experiments the material is implanted [2]. The purpose of this study was to investigate the ability of relevant bacterial strains, namely *S. epidermidis*, to adhere onto two distinct types of nanohydroxyapatite (nanoHA), sintered at 725°C and 1000°C, that are intended to be used as bone-regeneration material, and to evaluate how bacteria-nanoHA interactions are affected by the presence of a protein model, fetal bovine serum (FBS), which is a mixture of serum proteins.

METHODS: The bacterial strains used in this study were *S. epidermidis*; the reference type culture RP62A, a known slime producer and a clinical strain, isolated from an orthopaedic infection (*S. epidermidis* ORT). Samples with 10mm diameter of nanoHA (Fluidinova S.A., Portugal) were prepared by uniaxially pressing and sintering for 15 min at 725°C and 1000°C. The nanoHA samples; either bare or FBS coated, were placed in contact with 10^8 CFUs/ml of bacterial solution and incubated at 37°C, with gentle shaking, for 60 min. Subsequently, the adhered bacterial cells were observed by scanning electron microscopy (SEM), released by sonication and quantified as colony forming units (CFU). Contact angle measurements were performed to evaluate materials wettability.

RESULTS: Table 1 presents the contact angles on the various substrates. The low values obtained for all substrates indicate the presence of hydrophilic surfaces. Figure 1 shows that both *S. epidermidis* strains adhesion is significantly higher on nanoHA sintered at 725 ºC than on the one sintered at 1000 ºC. The presence of FBS on the nanoHA surface significantly reduced bacterial adhesion for both strains as compared with that measured on bare nanoHA, for both sintering temperatures.

Table 1. Contact angles (deg) (average ± SD) for nanoHA materials sintered at 725ºC and at 1000ºC with and without (control) adsorbed FBS.

Contact angle (deg)	Control (deg)	FBS (deg)
NanoHA 725	40,2 ± 3,9	32,7 ± 3,4
NanoHA 1000	38,3 ± 1,8	26,1 ± 1,8

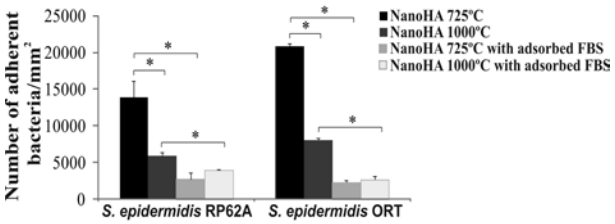

Fig. 1: Influence of adsorbed FBS on the bacterial adhesion to nanoHA sintered at 725ºC and at 1000ºC. Results presented are the average ± SD. Indicates significant differences ($p<0.05$).*

DISCUSSION & CONCLUSIONS: The higher surface area and porosity, as well as, the lower negative charge of the nanoHA substrate sintered at 725ºC [3] may explain the higher number of adherent bacteria on nanoHA725 samples as compared to nanoHA1000. The reduction of *S. epidermidis* adhesion on two distinct types of nanoHA in the presence of FBS may be due to the increased hydrophilicity of the surface. This study emphasizes the importance of the role played by proteins at the initial stages of bacterial adhesion.

REFERENCES: [1]M.G. Katsikogianni et al (2010) *Acta Biomaterialia* **6**:1107-18. [2]Y. Liu et al (2008) *Biomaterials* **29**:4374-82. [3]N. Ribeiro et al (2010) *J. Colloid Interface Sci*. **351** 398-406.

ACKNOWLEDGEMENTS: This work was financed by FEDER (COMPETE) and by FCT in the framework of the NaNOBiofilm (PTDC/SAU-BMA/111233/2009) and NanoforBone Project (NORTE-01-0202-FEDER-005372).

TiNOx coatings duplicate the effects of SLA"active"

P. Rieder, G. Garavaglia, A. Filieri, H.W.A. Wiskott and S. Durual

Laboratory of biomaterials, School of dental medicine, University of Geneva, CH

INTRODUCTION: Titanium Nitride Oxide (TiNOx) coatings are known for their biocompatibility, hardness and high resistance to corrosion and wear. Further, they can be applied by plasma vapor deposition onto a wide variety of metallic, mineral, or organic substrates.

It was previously shown *in-vitro* that TiNOx coatings applied onto SLA-roughened titanium surfaces increased human primary osteoblast proliferation by 1.5 times in the first two weeks after cells seeding, while still maintaining a high degree of cell differentiation.

Therefore, the objectives of the present study were (i) to determine whether these findings would translate into the enhanced osseointegration of TiNOx-coated implants *in-vivo* and (ii) compare the osseointegration of Ti-SLA and CoCr-SLA implants coated with TiNOx.

METHODS: 48 cylinders made of Ti-SLA, Ti-SLA-TiNOx and CoCr-SLA-TiNOx (R_a = 2.49 ± 0.34µm) were implanted into the lower jawbone of 8 Gottingen minipigs. The animals were sacrificed after 1 week, 2 weeks, 1 month and 3 months. Standard morphometric techniques were applied to determine bone-to-implant contact.

RESULTS: All implants healed uneventfully. None was lost and no unusual inflammation was noted. Osseointegration proceeded normally on all 3 surfaces, with equal activity after the first week of healing. After 2 weeks (fig. 1), bone-to-implant contact was 1.8 times higher on TiNOx coatings, either deposited on Ti or on CoCr (fig.2). These differences fell off after 1 and 3 months of healing.

CONCLUSIONS: When compared to standard SLA titanium, TiNOx coatings enhance implant osseointegration during the first month of healing, thereby duplicating the effect of SLA"active". Furthermore, this stimulating effect is independent of the substrate, leading to similar results whether the coating is applied onto SLA-titanium or onto SLA-CoCr.

ACKNOWLEDGEMENTS: This study was supported by a grant (659-2009) from the ITI foundation (ITI, Basel).

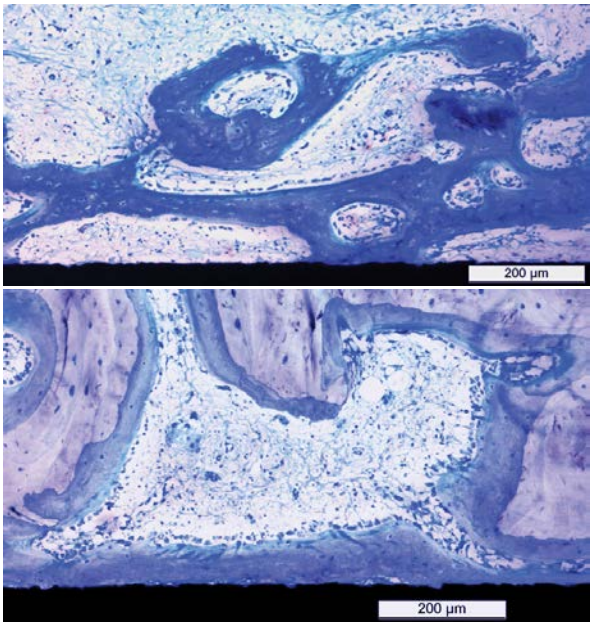

Fig. 1: High magnifications of Ti-TiNOx periimplant zones after 2 wks healing.

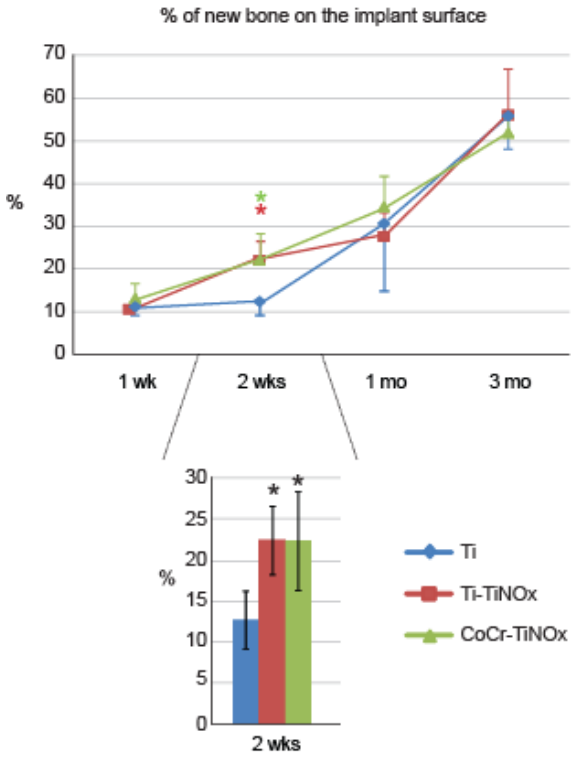

*Fig. 2: New bone-implant contact after 1 wk, 2 wks, 1 mo and 3 mos healing. Data are expressed as mean ± SE. *: significantly different ($p<0.05$) from the Ti implants at the same time.*

Revcel, a resorbable biomaterial as wound dressing

M Rottmar[1], M Richter[1], X Mäder[1], K Grieder[1], B von Rechenberg[2], K Nuss[2], E Zimmermann[3], S Buser[3], A Dobmann[3], J Blume[3], A Bruinink[1]

[1] EMPA St. Gallen, Lerchenfeldstr. 5, 9014 St. Gallen [2] CABMM Tierspital Zürich, Winterthurerstr. 260, 8057 Zürich 3 nolax AG, Eichenstr. 12, 6203 Sempach Station

INTRODUCTION: Chronic wounds of the skin, if at all, generally take very long to heal. They cause pain for the patients and treatment causes very high costs for the health care system. Worldwide an estimated 54 Mio patients suffer from chronic wounds, which number is expected to dramatically increase in the coming decades Stagnation of wound healing usually results in excessive extracellular matrix (ECM) degradation[1]. The ECM is, however, of crucial importance for tissue regeneration as a reservoir of growth factors and as a matrix for the ingrowth of cells into the wound.

Current concepts to treat chronic wounds include topical application of growth factors, stem cell and gene therapy approaches as well as application of natural or artificial scaffolds[2]. So far, however, most of the available cell adhesion-promoting scaffolds contain collagen, which has the potency to transmit pathogens or to elicit hypersensitivity[3]. In addition, the treatment costs with such scaffolds are usually very high. The aim of this project was to develop a biocompatible, degradable artificial ECM based on polyurethane that is soft, yet form-stable and that offers optimal pore size for angiogenesis and cell adhesion. The scaffold is expected to adjust to the wound bed after contact with body fluids preventing gaps between the scaffold and migrating cells.

METHODS: The Revcel materials were produced by nolax in a discontinuous procedure by mixing polyol and isocyanate together with other components. Generated block foams were cut into 0.8mm thin membranes for subsequent evaluation. Revcel extracts and degradation products were obtained based on procedures described in ISO 10993-1, -9, -12, -13 and -17. Toxicity of extracts and degradation products was assessed by measuring total protein content as well as metabolic activity according to ISO 10993-5. Cell adhesion was evaluated by cultivating 3T3 mouse fibroblast cells on the material followed by a staining for the actin cytoskeleton and nuclei.

RESULTS: Depending on the concentrations of the used hydrophilic components, Revcel formulations are variable in degradation time and foam structure. The release of potentially toxic constituents of 24h Revcel-extracts was evaluated by total protein content measurement. Materials with the base formulation (1008) showed low adverse effects as indicated by a small reduction in protein content while the subsequent modified formulations (1009-1014) affected protein levels to an even lesser extent. Therefore, the evaluated materials are considered to be non-toxic. In contrast to previously extracted (24h extraction) surfaces of Revcel base formulation (1008) on which cell cluster formation was observed within 24h, good cell attachment and spreading was seen on the modified formulation 1015 (Fig.1).

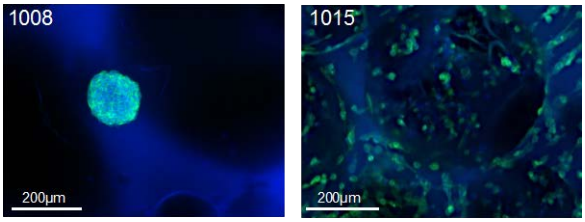

Fig. 1: Mouse 3T3 fibroblasts were cultivated on Revcel foams for 24h before staining for the actin cytoskeleton (green) and the nuclei (blue).

DISCUSSION & CONCLUSIONS: Revcel is a soft, synthetic, foam-like scaffold with optimal pore size for tissue ingrowth. Used as thin membrane, it can be easily cut according the wound bed size and shape. Depending on the exact formulation, the Revcel material is tunable in its degradation time. Material extracts as well as degradation products obtained by protocols reflecting the in vivo situation were found to be non-toxic. Furthermore, material formulations could be defined that show good cell attachment and spreading suggesting that Revcel has the potential to support wound healing in vivo.

REFERENCES: [1] G.S. Schultz and A. Wysocki, *Wound Rep Reg* (2009), 17 153–162; [2] V. Falanga, EWMA Journal (2004); 4(2): 11-13.[3] M.T.Madigan et al., Brock (2009), chapter 28, pages 822ff.

ACKNOWLEDGEMENTS: We acknowledge the support by the CTI (project 11874.1 PFLS-LS).

Cell instructive biomaterial design for enhancing cell contractility and osteogenic differentiation of mesenchymal stem cells

RI Sharma[1, 2], G Bartalena[1, 2], JG Snedeker[1, 2]

[1] *Department of Orthopedics, University of Zurich, Zurich, Switzerland,* [2] *Institute for Biomechanics, ETH Zurich, Zurich, Switzerland*

INTRODUCTION: Substrate based approaches to direct stem cell differentiation rely on cell-matrix interactions and related biochemical and mechanical cues, which can regulate cell signaling and differentiation [1-3]. We attempted to upregulate osteogenic differentiation on fibronectin and RGD using substrates with a range of mechanical compliance. We hypothesized that RGD fragments would increase efficiency of integrin mediated cell binding and substrate contraction compared to the full length molecule.

METHODS: Polyacrylamide substrates (Invitrogen) with mechanically reproducible compliances were coupled with either RGD or whole length fibronectin [4]. Cell attachment was assayed by normalizing cell counts after 1 hour. We quantified the expression of focal adhesion elements with RT-PCR. Cell morphology was examined by staining with FITC-phalloidin. Phosphorylated ROCK activity was assessed with a colorimetric ELISA. Osteogenic differentiation was examined by staining for mineralized deposits with Alizarin Red. RT-PCR confirmed osteogenic differentiation at the molecular level. In some cultures media was supplemented with Y27632, an inhibitor of ROCK, and differentiation was assessed. Finally, substrate contraction was measured in terms of strain by incorporating nanoreporter beads in the substrate.

RESULTS: Cell attachment assays revealed higher levels of attachment on RGD-functionalized substrates, and similarly focal adhesion elements on RGD functionalized substrates were expressed at higher levels. Cell morphology appeared stellate on fibronectin substrates, while those on RGD appeared well spread. Differentiation assays show more calcified nodules on RGD-functionalized substrates compared to fibronectin substrates, and this trend decreased with increasing compliance (Fig 1A-F). PCR confirmed the expression of osteogenic markers on RGD substrates. Inhibiting ROCK activity prevented nodule formation. Substrate deformation was reduced as the substrate compliance increased, but the presence of RGD facilitated substrate deformation (Fig 1G).

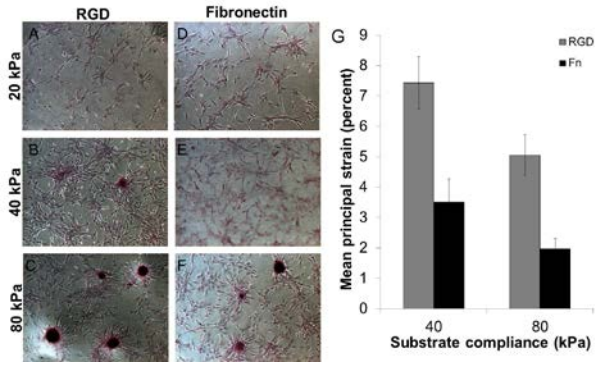

Fig. 1: (A-F) More mineral nodules were visualized on RGD substrates compared to fibronectin. (G) Strain was reduced with increasing substrate compliance but RGD functionalization allowed increased deformation.

DISCUSSION & CONCLUSIONS: Cell mechanics provides an alternate paradigm for directing cell differentiation. Our findings verify that interactions between substrate compliance and ligand chemistry (cell-matrix coupling) can have an additive effect. At the biophysical level, the ligand presentation on a deformable substrate is critical for the generation of integrin-driven substrate remodeling and signal transduction and ligand chemistry can be used to manipulate these. More generally, this study shows that strategic ligand choice could potentially be used to shift cell sensitivity to substrate stiffness and quantitative elucidation of the interactions between ligand chemistry and substrate mechanics are on-going.

REFERENCES: [1] R.I. Sharma and J.G. Snedeker (2010) *Biomaterials*, 31(30):7695-704. [2] A.J. Engler, et al (2006) *Cell* 126(4):677-89. [3] R.I. Sharma and J.G. Snedeker (2012) *PLoS One* 7(2):e31504. [4] R.J. Pelham and Y. Wang (1997) *Proc Natl Acad Sci U S A* 94(25):13661-5.

ACKNOWLEDGEMENTS: This work was funded by the Bonizzi-Theiler Stiftung. The authors thank Vincent Diederich from Massimo Morbidelli's group (Chemical Engineering, ETH Zurich) for continued collaborations to manufacture substrates for TFM studies.

Preparation and characterization of novel biodegradable nanoparticles for pharmaceutical applications

I. Altimari, M. Curcio, F. Iemma, U.G. Spizzirri, F. Puoci, N. Picci
Pharmaceutical Science Department, University of Calabria, Ed. Polifunzionale, Rende (CS) 87036, Italy. ilaria.altimari@unical.it

INTRODUCTION: In recent years, significant attempts have been devoted to the development of new nanoparticulate systems to be used as delivery devices of several drugs [1]. In particular, nanogel based on natural polymers are attracting much attention because of their possibility to obtain materials characterized by good properties in terms of biocompatibility and biodegradability. This work proposes a new solvent-free emulsion polymerization method to obtain biodegradable gelatin-based nanospheres as potential drug delivery devices.

METHODS: pH-sensitive nanospheres were synthetized by radical graft polymerization of gelatin with methacrylic acid sodium salt and N,N'-ethylenebisacrylamide, as pH-responsive monomer and crosslinking agent, respectively [2].

Sunflower seed oil and lecithin were employed as continuous phase and surfactant, respectively, to completely overcome any problems of toxicity related to the uses of potentially harmful organic solvents in the polymerization process. In order to determine the influence of the surfactant on the hydrogels performances, three different polymeric materials were obtained varying the amount of lecithin in the organic phase. These nanoparticles were characterized by scanning electron micrograph, particle size distribution and swelling experiments. Moreover, in order to test the suitability of the synthesized polymers as drug delivery devices, release experiments at pH 7.4 and in gastro-intestinal simulating fluids were performed using Diclofenac sodium salt, as model drug. Finally, enzymatic biodegradability tests, using pepsin and pancreatin solutions, were performed in order to verify the stability of the nanoparticles towards the enzymes of gastrointestinal tract.

RESULTS & DISCUSSION: The nanoparticles showed a spherical shape and a porous surface, confirming the suitability of the proposed polymerization procedure to obtain spherical materials. Dimensional analyses showed that the particle diameter decreases as the amount of surfactant enhances. Moreover, water uptake experiments, performed at pH 1.0 and 7.4, demonstrated the dependence of the pH medium on the swelling properties. The higher water affinity at pH 7.4, compared to pH 1.0, is ascribable to the electrostatic repulsions of dissociated carboxylic pendant groups in the hydrogels. Drug release experiments in gastrointestinal simulating fluids showed that drug release percentages are strongly affected by the pH variations of the medium. At pH 1.0 the acidic groups are undissociated and low amounts of drug are released. After 2h, when pH jumps to 7.4, the hydrogels swell because of the repulsion of negative charges of carboxyl groups and the drug molecules easily diffuse through the polymeric structure. Biodegradability tests in pepsin demonstrated no significant weight loss, while, when incubated in pancreatin solution, an increasing of the polymer degradation rate as the particle size decreases was verified. The influence of particle size on the degradation can be ascribable to the fact that, in smaller particles, the products of degradation forming during the degradation process can diffuse easily to the surface, while in the larger particles degradation products have a longer path to the surface of the particle.

CONCLUSIONS: In this work a new polymerization method to obtain gelatin-based spherical particles able to respond to pH variations was presented. The influence of the surfactant concentration on the particle size and shape was investigated, and the real applicability of the nanospheres as drug carriers demonstrated.

REFERENCES: [1]M. Hamidi, A. Azadi, P. Rafiei (2008) *Adv Drug Del Reviews* **60**:1638-16492. [2]U.G. Spizzirri, F. Iemma, I. Altimari et al (2012) *J Mater Sci* **47**:3648–3657.

ACKNOWLEDGEMENTS: This study was financially supported by thev MIUR (Programma di ricerca di rilevante interesse nazionale 2008) and the University funds.

Biomimetic fibrinogen-hyaluronan conjugates for nucleus pulposus regeneration

Z Li[1], R Sirkis[2], M Peroglio[1], A Wertzel[2], K Mevorat-Kaplan[2], M Alini[1], A Yayon[2], S Grad[1]

[1] *AO Research Institute, Davos, Switzerland.* [2] *Procore laboratories, Nes Ziona, Israel*

INTRODUCTION: Degenerative disc disease is one of the largest health problems faced worldwide. With age, the water content of the nucleus pulposus (NP) decreases and the disc gradually becomes less effective as a cushion. As a result, mechanical load on the annulus fibrosus (AF) leads to weakening of the AF and eventually to its cracking through which part of the gelatinous NP may prolapse. The IVD does not possess self-repair capacity. A novel nano-biopolymer conjugate: Hyaluronic acid (HA)-Fibrinogen (FBG) Protein Link (HPL) was developed to mimic native extracellular matrix for minimally invasive disc regeneration treatment. The present study aimed to evaluate different formulations of HPL for their ability to provide an optimal three dimensional environment for NP cell growth and differentiation.

METHODS: HPL at different FBG:HA ratios (2, 4) and HA molecular weights (B, C) were supplied by Procore Ltd, IL. P1 bovine NP cells (NPCs) were seeded into HPL gel beads at a density of 120,000 cells per bead. Each bead was prepared using 20 µL of HPL solution and 10 µL of thrombin (1U/mL final concentration) to cause gelation. Cell-gel constructs were cultured in DMEM + 10% FCS + 50 µg/mL ascorbic acid for 3, 7 or 14 days. Constructs of pure FBG and non-conjugated FBG-HA mixtures were cultured as controls.

Outcome measurements included Live/Dead staining, histology , DNA and glycosaminoglycan (GAG) content, and mRNA expression of collagen type I and II, aggrecan, Sox9, carbonic anhydrase 12 (CA12), keratin 19 (KRT19), and biglycan (BGN).

RESULTS: Live/Dead assay showed that more than 95% of the cells were viable at all time points. The DNA content of FBG and FBG-HA mixture gels decreased over time, compared with HPL gels, which demonstrated consistent DNA amounts, suggesting improved stability of the HPL constructs.

Toluidine Blue staining on all time points showed rounded cells in the HPL gels, FBG and FBG-HA mixture indicative of an NPC-like phenotype. In all materials, bNPCs accumulated more at the edges. The extracellular matrix accumulation was also more intense at the edges of gels.

There was more accumulation of GAG in HPL compared to FBG or FBG-HA mixtures. HPL B2 showed least degradation and retained the highest GAG by day 14 (Fig. 1).

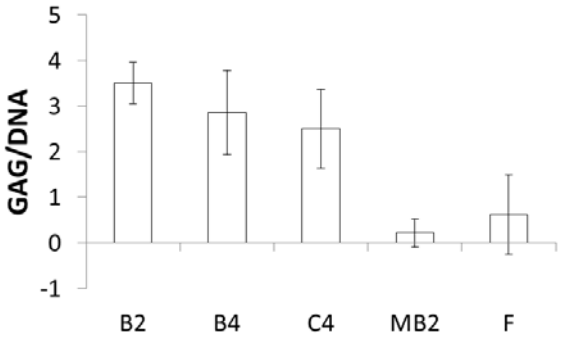

Fig. 1: GAG/DNA value in hydrogels after 14 days of culture. B2, B4, C4: HPL gels; MB2: FBG-HA mixture; F: FBG. Mean±SD, n=6.

There was a trend for highest gene expression of collagen II and transcription factor Sox9 in HPL B2 conjugates. A decrease in aggrecan and collagen II expression was observed during culture, while the NP markers carbonic anhydrase 12, keratin-19 and biglycan were maintained or up-regulated in all materials.

DISCUSSION & CONCLUSIONS: HPL provides the cells with a 3D environment made of HA as a major natural matrix component of the NP, and FBG, which facilitates gelation and provides stability. The present study indicates that HPL is capable of supporting NPCs retention and growth while retaining at least partially their differentiated phenotype. HPL may be suitable as injectable hydrogel for biological NP regeneration. A more extensive study will be required to establish whether there are significant differences in NPC activity between different HPL formulations.

ACKNOWLEDGEMENTS: Funded by the European Commission under the FP7 – NMP Project NPmimetic.

Hydrogels for BMP-2 delivery: Influence of carrier nature and pH on ectopic bone formation

Ludmila Luca[1], Anne-Laure Rougemont[2], Beat H Walpoth[3], Robert Gurny[1], Olivier Jordan[1]

[1] *School of pharmaceutical sciences, University of Geneva, University of Lausanne, Geneva, CH,* [2]*Division of Clinical Pathology and* [3]*Cardiovascular Research, Geneva University Hospital, Geneva, CH*

INTRODUCTION: Bone morphogenetic protein-2 (BMP-2) may be used in bone repair to circumvent limitations of autologous bone grafting. Therapeutic BMP-2 application requires a carefully designed delivery carrier to prevent rapid clearance from the application site and preserve protein function. A potential pitfall lies in rhBMP-2 bioactivity loss due to conformation and aggregation changes close to the physiological pH [1]. Two biopolymers are attractive carrier options: hyaluronic acid (HY) and chitosan (CH). The objective of the present work is to compare the osteoinductive activity of rhBMP-2-loaded CH and HY carriers in a rat ectopic bone induction model at two different pH [2].

METHODS: A new injectable chitosan hydrogel that forms *in situ* a biodegradable gel [3] and a commercial cross-linked hyaluronan were used. Hydrogels loaded with 145 µg rhBMP-2 (Inductos®, Wyeth Pharmaceuticals) were prepared at pH 4.8±0.2 and 6.2±0.2. CH and HY hydrogels, loaded or not with rhBMP-2, were injected in rat quadriceps of Sprague-Dawley rats (n=6). Mineralized bone volume (MBV) was assessed at 3 weeks by microCT-scan and histopathology. Paired Wilcoxon test at $p<0.05$ level were used for analysis.

RESULTS: Bone formation was observed at 3 weeks with both carrier types at both pH values. Controls devoid of rhBMP-2 did not induce bone. Higher bone formation was observed at low pH (4.8) compared to high pH (6.2), with ratio $MBV_{low\ pH}/MBV_{high\ pH}$ significantly higher than unity. HY hydrogel demonstrated a significantly higher bone formation compared to the CH hydrogel. Histopathological analysis demonstrated both trabecular and woven bone surrounding a hematopoietic bone marrow, with congestive vessels. No remains of injected chitosan hydrogel were detected. In contrast, hyaluronan hydrogel was not completely resorbed.

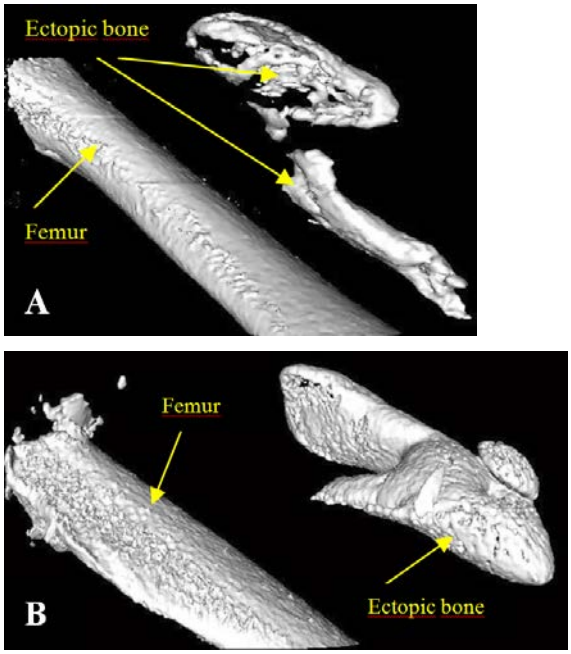

Fig. 1: CT-scan surface rendering showing ectopic bone at 3 weeks induced by 150 µg rhBMP-2 in chitosan (A) and hyaluronic acid (B) hydrogels at pH 4.8

DISCUSSION & CONCLUSIONS: The present study highlights the importance of the carrier's characteristics such as formulation pH and nature for osteoinductive activity of rhBMP-2. The rhBMP-2 bioactivity decreased at high pH probably due to protein aggregation and/or conformational changes [1]. The higher rhBMP-2 bioactivity in HY hydrogel might be explained by higher protein retention at the injection site due to the ionic complexation of the protein with HY and slower resorption of HY hydrogel compared to CH hydrogel.

REFERENCES: [1] L. Luca et al (2010) *Int J Pharm* **391**:48-54 [2] L. Luca et al (2010) *J Control Release* **147**:28-44; [3] E. Patois et al (2009) *J Biomed Mat Res* **91**:324-330; [4] L. Luca et al (2011) *J Biomed Mater Res A* **96(1)**:66-7

Encapsulation of Huh-7 cells within alginate-poly(ethylene glycol) hybrid microspheres

R Mahou[1], NM Tran[2], M Dufresne[2], C Legallais[2], C Wandrey[1]

[1]SV-IBI-LMRP, EPFL, Lausanne, Switzerland. [2]CNRS UMR 6600 Biomécanique et Bioingénierie, Université de Technologie de Compiègne, France

INTRODUCTION: Sodium alginate (Na-alg) is studied as raw material for numerous biomedical applications including cell immobilization in hydrogel microspheres intended for subsequent transplantation. However, microspheres obtained by ionotropic gelation frequently suffer from mechanical stability deficiency, limited durability, and permeability drawbacks. Coating or reinforcement of the initially formed beads with polycations requires multi-step processes and can have unwanted negative impacts on the biocompatibility. Considering the requirements of efficient cell microencapsulation, novel calcium alginate-poly(ethylene glycol) hybrid microspheres (Ca-alg-PEG) have been prepared by combining ionotropic gelation of PEG-grafted sodium alginate (Na-alg-PEG) and covalent cross-linking via disulfide bond formation.

METHODS: Heterobifunctional PEG was synthesized by alteration of the terminal hydroxyl groups of PEG and subsequently grafted onto Na-alg.[1]

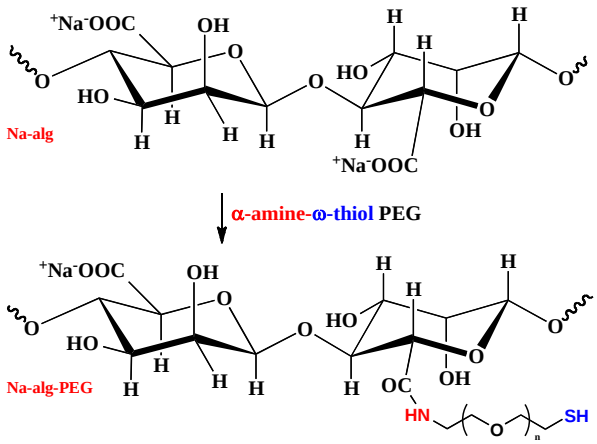

Fig. 1: Grafting of α-amine-ω-thiol PEG onto Na-alg resulting in Na-alg-PEG.

RESULTS & DISCUSSION: Grafting up to 13% of the Na-alg with α-amine-ω-thiol PEG did not affect the ability to form physical hydrogels in presence of Ca^{2+}. Moreover, the conjugated reactive thiol end groups allowed for simultaneous chemical cross-linking via disulfide bonds yielding hybrid hydrogels (Ca-alg-PEG).

Human hepatocellular carcinoma cells (Huh-7) were encapsulated in Ca-alg-PEG and cultured for two weeks.[2]

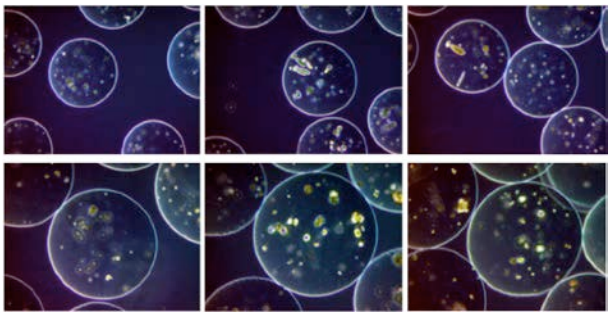

Fig.2: Microencapsulated Huh-7 cells within (top) Ca-alg and (bottom) Ca-alg-PEG. (from left to right) at days 1, 7 and 14.

Huh-7 cells encapsulated within Ca-alg-PEG continued proliferation up to 14 days, suggesting no detrimental effect of the encapsulation procedure on the ability of cells to proliferate (Fig. 2). Ca-alg-PEG thus offers favourable environmental conditions for cell viability and proliferation, even slightly better than Ca-alg. Cells encapsulated in Ca-alg-PEG form multi-cellular structures and spheroid aggregates. Besides the survival and proliferation, albumin production by encapsulated Huh-7 cells continued, similar secretion of albumin within Ca-alg-PEG and Ca-alg was observed. This production remained almost constant over time during the studied period, up to two weeks.

CONCLUSIONS: The novel calcium alginate-poly(ethylene glycol) hybrid microspheres seem to overcome the physical drawbacks of Ca-alg but, at the same time, conserve the favourable microsphere properties necessary for biomedical applications.

REFERENCES: [1]Mahou et al (2012) *Polymers* **4**:561-589. [2]Mahou et al (2012) *J. Mater Sci-Mater Med* **23**:171-179.

ACKNOWLEDGEMENTS: The authors thank the Swiss National Science Foundation for financial support (Grants 205320-130572/1 and 205321-116397/1).

Bone cements for localized treatment of tumors through combined hyperthermia and chemotherapy

M Mohamed[1], V Bernau[2], H Hofmann[2], G Thalmann[3] G Borchard[1], O Jordan[2]

[1] *School of Pharmaceutical Sciences, University of Geneva, University of Lausanne, Geneva, CH.* [2]*Laboratory for Powder Technology, Ecole Polytechnique Fédérale de Lausanne (EPFL), Lausanne, CH.* [3] *Insel Hospital, Department of Urology, Bern, Switzerland*

INTRODUCTION: Bone metastases might be efficiently treated using intraosseous implants. In this view, we propose novel formulations that, once injected intraosseously, form a solid implant. Poly(methylmethacrylate) cements (PMMA) are relevant formulations already used in vertebroplasty. They can be loaded with both an anticancer agent (doxorubicin DOX) and superparamagnetic silica beads (SSB) for combining chemotherapy and hyperthermia, the latter being an effective adjuvant in cancer therapy.

METHODS: Cement was prepared by mixing poly(methylmethacrylate) and its monomer in presence of an initiator and an activator. SSB at 24% or 30% (w/w) and DOX at 2.5% (w/w) were loaded within the cement. Heating capacity was assessed by measuring cement temperature increase under an external alternating magnetic field (6 mT and 140 kHz). *In vitro* DOX release was carried out in a saline media at 37°C and the DOX was analyzed by spectrophotometry at 479 nm. *In vitro* toxicity of the implants was tested using XTT proliferation assay. Immortalized human prostate cancer cells, PC3, were incubated for 24h before the cell viability was measured and compared with a control of non-treated cell. Young modulus was determined by compression of Ø6x7 mm cylinders.

RESULTS: PMMA cement was able to generate heat in the range of 43-44 °C and displayed sustained release over at least 10 days. The release profiles were not influenced by the heat generated during a 25 min-hyperthermia session at 6 mT and 140 kHz, allowing further studies on the synergetic effects of hyperthermia and chemotherapy. The heating power of the implants, so-called specific power loss (SPL), indicates the potential for hyperthermia-induced antitumoral effect. Cement for intraosseous injection might provide some mechanical support to the weakened bone as the Young compression moduli are in the range of cancellous bone. *In vitro* toxicity of eluted DOX on PC3 cells shows preserved drug cytotoxicity.

Table 1. Characteristics of acrylic cements

	Cement	Cement-SSB 24% (w/w)	Cement-SSB 30% (w/w)
Elasticity [MPa]	186.1 ± 62.6	367.6 ± 130.6	239.1
SPL* [W/g]	-	1.97 ± 0.04	2.13 ± 0.06

***at 6mT**

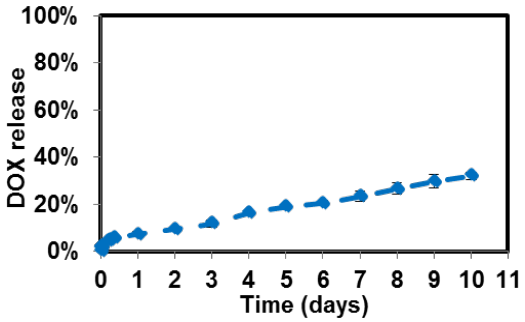

Fig. 1: DOX release profile of PMMA cement loaded with 24% SSB.

DISCUSSION & CONCLUSIONS: Acrylic cement was successfully loaded with doxorubicin and superparamagnetic nanoparticles, providing a sustained anticancer agent delivery and potential cytotoxic temperature. These data show within clinically acceptable parameters the feasibility of combining SPIONs for hyperthermia with local anticancer agent release.

ACKNOWLEDGEMENTS: Financial support was provided by the Swiss National Science Foundation (SNSF).

Encapsulation of antimicrobial compounds into inorganic nanocontainers

M. Priebe, K. M. Fromm

Department of Chemistry, University of Fribourg, Chemin du Musée 9, CH-1700 Fribourg, Switzerland

INTRODUCTION: Nanometer sized hollow spheres, called nanocontainers, exhibit an emerging potential as they can be used as drug carriers, reactors, confined reaction vessels, etc. Not only guest molecules can be enclosed inside their empty interior, but the shell of the capsule also provides additional protection [1,2]. The microemulsion method approach is superior to the traditional methods since micelles are used instead of solid templates. Reaction between reagents on the boundary phase between a micelle and the surrounding phase leads to the formation of a nanocontainer [3]. The aim of this project is to encapsulate an antimicrobial silver coordination polymer inside inorganic nanocapsules.

METHODS: Inorganic nanocontainers such as CuS, TiO_2 and SiO_2 are prepared both in oil-in-water and water-in-oil microemulsions[1-4]. Nanoparticles are characterized using TEM, HRSEM, EDS, XRPD and DLS. Under high vacuum, solutions of silver-binding ligand and $AgNO_3$ are intended to penetrate through the pores in the wall into the hollow spheres. The size of the resulting complex should prevent spontaneous leave from the capsule. The incorporation process will be followed by TGA and IR.

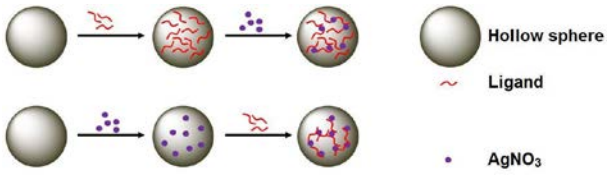

Fig. 1: Schematic illustration of the incorporation of a silver-binding ligand and $AgNO_3$ into the hollow spheres.

RESULTS: HRSEM and TEM demonstrated well-defined spherical particles. Increased electron density on the border of the particles indicated the presence of their hollow nature. The size of CuS, TiO_2 and SiO_2 containers differed depending on the material and reaction conditions exhibiting the outer diameter 40-50, 500-2000 and 50-120 nm, respectively.

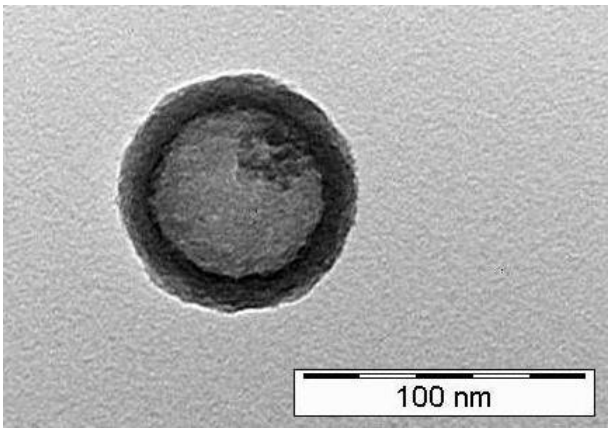

Fig. 2: TEM image of a SiO_2 nanocontainer prepared in water-in-oil microemulsion..

DISCUSSION & CONCLUSIONS: Inorganic nanocontainers prepared in the micromulsion system have been successfully synthesised. The biggest challenge, however, is the reproducibility of the results due to the sensitivity of microemulsions to even a slight change in the reaction conditions. Silica nanocapsules have been chosen for the incorporation of antimicrobial compounds since depending on the purification parameters wall thickness and pore size can be tuned. Further investigations will include the improvement of encapsulation techniques and subsequently antimicrobial and cytological assays.

REFERENCES: [1] Y.-S. Lin, S.-H. Wu, C.-T. Tseng et al (2009) *Chem Commun* 3542–3544. [2] S.-H. Wu, C.-T. Tseng, Y.-S. Lin et al (2011) *J Mater Chem* **21**:789–794. [3] H. Gröger, F. Gyger, P. Leidinger et al (2009) *Adv Mater* **21**:1586–1590. [4] A.M. Collins, C. Spickermann, S. Mann (2003) *J Mater Chem* **13**:1112-1114.

ACKNOWLEDGEMENTS: We are grateful to the Swiss National Science Foundation, the NRP-62, the University of Fribourg and the FriMat for generously supporting this project.

The effect of material choice on the immune response to bacterial contamination

ETJ Rochford[1,2], AHC Poulsson[1], L O'Mahony[3], M Ziegler, RG Richards[1,2], TF Moriarty[1]

[1]AO Research Institute, AO Foundation, Davos, CH. [2]IBERS, Aberystwyth University, UK, [3]Swiss Institute of Allergy and Asthma Research (SIAF), University of Zurich, CH

INTRODUCTION: The presence of an implanted biomaterial compromises the immune system and increases infection risk[1]. Previously it has been shown that different materials induce different immune responses, which may influence susceptibility to infection[2]. In the current study a range of orthopaedic biomaterials, with and without bacterial contamination, have been examined to identify the role of material choice in the immune response to infection *in vitro*.

METHODS: Materials: The following materials were used in this study to compare different surface chemistries and topographies: micro-rough titanium (TS), electropolished titanium (TE), Titanium-Aluminium-Niobium (NS), electropolished Titanium-Aluminium-Niobium (NE), stainless steel (SS)[a], injection moulded polyetheretherketone(PEEK) (PO), machined PEEK (PA) and oxygen plasma treated PO (PO30) and PA (PA30)[b] as previously described[3]. For experiments requiring adherent bacteria, approximately $2x10^5$ *Staphylococcus aureus* JAR cm^{-2} were adhered to the materials using a bacterial adhesion chamber[3]. All experiments were performed in triplicate.

Complement Activation: The activation of complement by the materials with and without pre-adhered *S. aureus* JAR was assessed by exposing the samples to human serum for one hour and measured using a C3a-desArg ELISA.

Leukocyte Stimulation: THP-1 monocyte cells were used to screen for NF-κB activation by the materials using the Quanti-blue assay with and without additional lipopolysaccharide (LPS) stimulation. Additionally, peripheral blood mononuclear cells (PBMC) were isolated from healthy donors and exposed to the materials, the materials and LPS or the materials pre-contaminated with *S. aureus* JAR for 48 hours. The PBMC were harvested for real-time PCR and samples of the cell media taken for multiplex analyte detection by Bioplex. The Bioplex screened for IL-8, IL-10, IL-12(p70), TNF-α, MIP-1α and G-CSF.

RESULTS: In general, TS produced the lowest level of immune-activation as illustrated by the complement (Fig.1), NF-κB and cytokine assays in the absence and presence of bacteria. In contrast, PEEK was generally the most stimulatory of the materials; increasing complement activation, NF-κB, IL-12 and TNF-α secretion. Interestingly oxygen plasma treatment led to increased complement activation (Fig.1), TNF-α and IL-12 production but decreased NF-κB stimulation in the presence of bacteria or LPS. MIP-1α secretion was dependent on the material, though no clear trend for material classes could be identified (Fig.2).

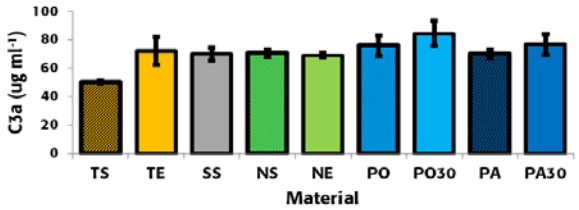

Fig.1: Complement activation by the different materials without additional stimulation(n=3,±s.e)

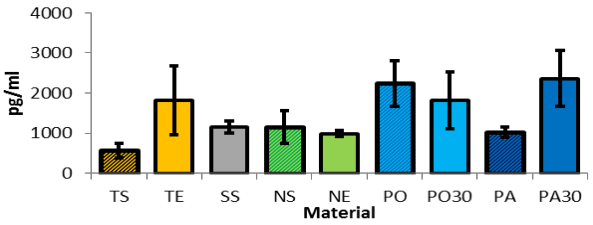

Fig.2: MIP-1α secretion by PBMCs exposed to the materials coated with S. aureus JAR(n=3,±s.e.)

DISCUSSION & CONCLUSIONS: There may be differences in the immune response to materials due to surface chemistry, particularly between TS and PEEK. Interestingly, chemokine production was the most differentially induced of the analytes measured. These differences may affect the ability of the immune system to respond to infection. Roughness, however, did not have a consistent effect on the immune response. To understand how these differences affect the immune response to bacterial contamination of an implant in a trauma wound deserves further *in vivo* investigation.

REFERENCES: [1] S. Elek and P. Conen (1957) *Br J Exp Pathol* **38**:573-586. [2] J.J. Boelens et al (2000) *J Infect Dis* **181**:1337-1349. [3]E.T.J. Rochford et al (2011) ESB2011.

ACKNOWLEDGEMENTS:[a]Metal samples from Synthes, [b]PEEK samples from Invibio Biomaterial Solutions.

Chemical stability of ultraviolet-ozone treated, injection-moulded poly lactic acid micro-cantilevers

Prabitha Urwyler[1], Alfons Pascual[2], Jens Gobrecht[2,3,4], Helmut Schift[3,4], and Bert Müller[1]

[1] Biomaterials Science Center, University of Basel, Basel, CH. [2] Institute of Polymer Engineering, University of Applied Sciences and Arts FHNW, Windisch, CH. [3] Laboratory for Micro- and Nanotechnology, Paul Scherrer Institut, Villigen PSI, CH. [4] Institute of Polymer Nanotechnology, University of Applied Sciences and Arts FHNW, Windisch, CH.

INTRODUCTION: Polymers including poly lactic acid (PLA) are widely used in the area of bio-analytics and bio-sensing. Micro injection moulding (µIM) belongs to the promising methods for mass fabrication of polymeric biosensors, such as micro-cantilevers (µCs) [1]. Injection moulded µCs have been successfully applied for sensing bio-molecular interactions [2]. Clean surfaces are a pre-requisite for sensing interactions. Ultra-violet ozone (UVO) treatment, which is used as a standard procedure for cleaning, may degrade the polymer material and hence needs to be studied.

METHODS: PLA µCs were manufactured using µIM as described earlier [1]. The surface of the PLA µCs was treated in the UVO cleaner (UV Clean Model 13550, Boekel Scientific, Feasterville PA). The PLA µCs were treated for a period of 30 minutes. Changes to the material's surface were investigated by reflection Fourier transform infrared spectroscopy (FT-IR). FT-IR spectra of two areas of the cantilever holders were performed using a Centaurus IR-microscope coupled to a Nexus IR spectrometer (Thermo Electron, Thermo Fisher Scientific, Dreieich, Germany) with a grid of 300 µm × 300 µm. The material was examined for changes using a Differential Scanning Calorimeter (DSC). The entire µC array along with the holder was thermally analyzed with DSC (DSCQ1000, TA Instruments, Waters GmbH, Eschborn, Germany). The recordings consisted of a first heating cycle from 0 to 250 °C, subsequent cooling to 0 °C and a second heating cycle again to 250 °C, in dry nitrogen atmosphere.

RESULTS: The FT-IR spectra of starting status and of 30 minutes UVO-exposed PLA specimens were almost identical. However, a slight decrease in the intensity of the ester signals (1250 to 1050 cm^{-1}) after irradiation was observed. The DSC recordings allowed the evaluation of the glass transition temperature (T_g) during the cooling phase and the second heating phase. A significant reduction in T_g by about 4 K was found indicating a chemical aging of the PLA specimen.

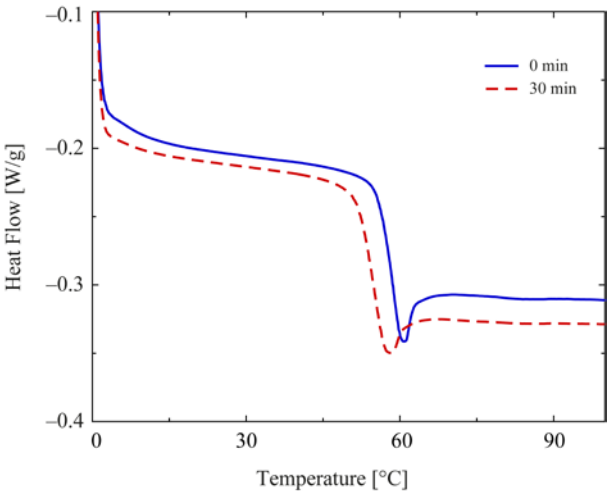

Fig. 1: The DSC analysis shows a significant decrease of the glass transition temperature after 30 minutes of ultraviolet-ozone exposure.

DISCUSSION & CONCLUSIONS: UVO-treatment as a surface cleaning method can significantly influence the properties of PLA µCs. We observed chemical aging after 30 minutes UVO-exposure [3].

REFERENCES: [1] P. Urwyler, H. Schift, J. Gobrecht et al (2011) *Sensors Actuators A* **33**:1471-77. [2] P. Urwyler, J. Köser, H. Schift et al (2012) *Biointerphases* **7**:8. [3] P. Urwyler, A. Pascual, P.M. Kristiansen et al (2012) *J Appl Polym Sci* In Press.

ACKNOWLEDGEMENTS: Financial support was provided by the Swiss Nanoscience Institute (SNI-project 6.2 DICANS). Technical assistance from members of PSI (LMN-INKA), FHNW (O. Häfeli) and EMPA (K. Jefimovs) is greatly acknowledged.

Electrospun scaffolds for annulus fibrosus repair. A scanning electron microscopy study.

N Wismer[1], S Thöny[1], G Fortunato[2], S Ferguson[3], S Grad[1] and D Eglin[1]

[1] AO Research Institute, Davos, CH. [2] Empa, St. Gallen, CH .[3] Institute for Biomechanics, ETH Zurich, Zurich, CH.

INTRODUCTION: The application of an electrospun membrane patch, which mimics the annulus fibrosus (AF) collagen fibers organisation and is seeded with a relevant cell source, is a promising method for AF tissue repair. Using scanning electron microscopy (SEM), this study aimed to evaluate the structural properties of electrospun polymeric scaffolds and their influence on AF cells seeding efficiency.

METHODS: Poly(ester-urethane) (PU, Mn=500'000 g/mol) produced as already reported and Poly(ε-caprolactone) (PCL, Mn=80'000 g/mol) purchased from Aldrich (Sigma-Aldrich) were processed into non-oriented and oriented electrospun scaffolds[(1,2)]. Bovine AF cells were seeded on top of scaffolds (7.8 x 10^4 cells/cm^2) and incubated (37°C, 5% CO_2, 90% humidity) in DMEM culture medium containing 10% FBS. The DNA content at day 1 on scaffolds relative to day 0 (initial seeded cells), reported as the seeding efficiency value in %, was measured spectrofluorometrically using the Hoechst 33258 dye assay (n=5). *SEM analysis*: Surfaces and cross-sections of the materials were prepared. Cross-sections were obtained by fracturing using a home-made holder after soaking into methanol and immersion in liquid nitrogen. Cell-seeded scaffolds were primary fixed in 2.5% glutaraldehyde and post fixed in 2% osmium in 0.1 M pipes. Then, scaffolds were sequentially dehydrated in ethanol before critical point dried (Quorum Technologies Ltd). All samples were mounted on Al stubs with silver paint; sputter coated with gold/palladium (10 to 20 nm) and evaluated using a SEM, Hitachi S-4700. For cross-section imaging, the SEM was operated at 1.5 kV, 20 µA and a working distance (WD) of 2-3 mm in a secondary electron (SE, -5 kV) detection mode. For cells seeded imaging, two SEM images were taken with introduction of a 4° tilt to produce a stereo pair of each image. The SEM was operated at 1.5 kV, 20 µA and a WD of 2.5 mm in a SE detection mode. The difference in parallax of each image was used to generate the 3-D image using Quartz PCI® software. Image analysis software (Axiovision® Software) was used to quantitatively analyse scaffolds (n=8). Fiber diameter and fiber orientation were assessed by evaluating 20 fibers in each surface image with a pixel size of 0.1 µm.

RESULTS: Both PU and PCL could be electrospun into scaffolds. PU fiber diameter (0.92 ± 0.35 µm) is smaller than the one of PCL (2.93 ± 1.53 µm) which results in a denser structure. The seeding efficiency values are 92 ±16 and 144 ±52 % on non-oriented and oriented PU scaffolds respectively. They are higher than on the PCL scaffolds irrespective of the orientation (47 ±12 %). Improved seeding distribution (depth) is observed for the non-oriented PCL scaffold compared to the PU and oriented PCL scaffolds.

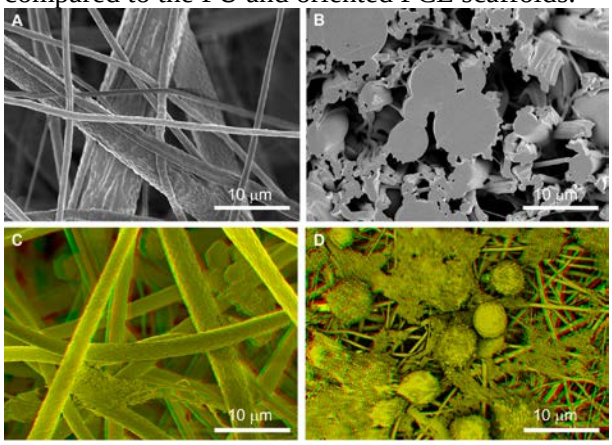

Fig. 1: SEM images of non-oriented PCL scaffolds surface (A) and cross-section (B), and surfaces of non-oriented PCL (C) and PU (D) scaffolds SEM red–green anaglyph after 1 day of seeding.

DISCUSSION & CONCLUSIONS: SEM analysis coupled with the DNA content indicates that although the PU scaffolds have improved AF cell attachment, the tight sub-micron fiber mesh is not effective for initial in depth cells ingrowth. Larger interconnected porosity in PU scaffolds is needed for cells ingrowth.

REFERENCES: [1]C.I. Boissard, PE. Bourban, AE. Tami et al (2009) *Acta Biomater* **5**:3316-27. [2]A.G. Guex, F. Kocher, G. Fortunato et al (2012) *Acta Biomater* **8**:1481-9. [3]C.M. Haller, G. Fortunato, T.P. Carrel et al (2008) *Int J Artif Organs* **31**: 601.

Magnesium corrosion associated gas cavity formation imaged *in vivo* using MRI

F Witte[1], K Kalla[1], M Meier[2]

[1] CrossBIT - Center for Biocompatibility and Implant-Immunology, Hannover Medical School, Germany. [2] Institute of Laboratory Animal Science, Hannover Medical School, Germany

INTRODUCTION: During fast corrosion of magnesium implants the formation of gas cavities is reported [1]. Even though methods to control and reduce fast magnesium corrosion *in vivo* has been established, it is not known how and where gas cavities are formed *in vivo* during fast magnesium implant corrosion [2]. This is mainly due to the fact that current analytical non-destructive *in vivo* methods such as ultrasound and *in vivo* µCT based methods have limitations and are not suitable. Here we demonstrate to use MRI based methods to follow gas cavity formation which even allows time-dependent quantification of the cavities.

METHODS: All animal experiments were conducted to according to NIH and animal welfare guidelines following an approved protocol from an ethical committee (33.12-42502-04-08/1499). Into the right femur of 3 mice a high purity Mg rod (99.99%, Good fellow) of about 250 µm thickness and 3 mm length were intramedullary implanted while the left femur was used as control. The mice were imaged by MRI immediately after surgery, 5 and 10 days, respectively. The mice were placed into the MRI in an animal bed with mask for gas anaesthesia and temperature controlled warming blanket. The gas anaesthesia has been performed with Isoflurane (1-2%) in oxygen using a Small Animal Monitoring System (Model 1025, SA Instruments, Inc.) for control of respiration rate, temperature, ECG and respiration triggering.

MRI was performed on a Bruker Pharmascan 70/16 (Bruker Biospin, Ettlingen, Germany) with a 16 cm horizontal bore magnet and a 9 cm (inner diameter) shielded gradient, 1H-resonance-frequency of 300 MHz and a maximum gradient strength of 300 mT/m. Data acquisition and image processing was undertaken with Bruker software Paravision 5.1 [3]. For segmentation image data were used to semi-automatically measure and reconstruct volumes of different tissues using ITK-Snap, a public domain segmentation tool [3].

RESULTS: Unique Ultrashort-TE imaging is able to detect even the low signal of bones and can enhance the precision of the detection of the implant position and gas cavities.

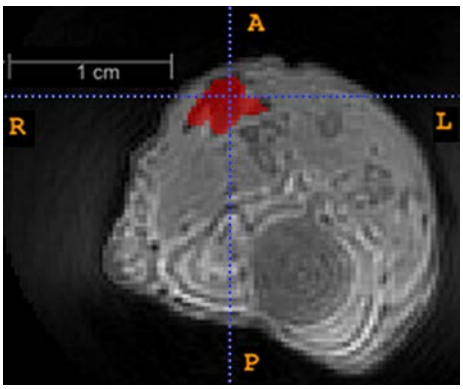

Fig. 1: Ultrashort TE Image of a mouse with a Mg implant in the right femur and gas cavity above the implantation site.

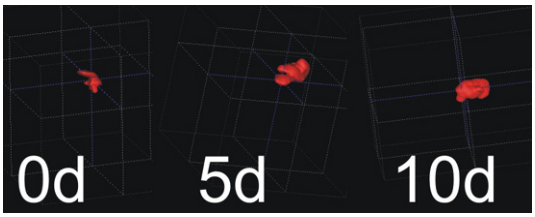

Fig. 2: Segmentations of the same gas cavity from left to right at consecutive time points (after surgery = 0, and after 5 and 10 days).

Table 1. Calculated volumes from semiautomatic segmentation of lesioned tissue.

	# Voxels	Volume (mm^3)	Mean (image)	S.D. (image)
0d	2128	55.94	5026.75	3449.82
5d	5999	157.69	3529.15	2482.05
10d	3071	80.72	3524.36	2569.79

DISCUSSION & CONCLUSIONS: It has been be demonstrated that Ultrashort-TE imaging provides a suitable method to consecutively image and quantify Mg corrosion associated gas cavity formation in soft tissues as a true *in vivo* method.

REFERENCES: [1] F. Witte et al (2008) *COSSMS*; **12**:63-72. [2] F. Witte et al (2010) *Acta Biomaterialia* **6**(5):1792-1799. [3] Yushkevich et al. (2006) *Neuroimage* **31**(3):1116-28.

Basic setup for microtomography of biosamples under cryo conditions.

F Witte[1], E Willbold[1], W Czayka[2], J Nellesen[2], W Tillmann[2]

[1] *Laboratory for Biomechanics and Biomaterials, Orthopaedic Clinic, Hannover Medical School, Germany.* [2] *Institute of Materials Engineering, Technische Universität Dortmund, Germany*

INTRODUCTION: Three-dimensional (3D) structural information of biological samples is a key issue to understand the complex cellular organization of tissues. However, to extend the analysis from marco to a cellular level, special histological and biochemical techniques are necessary. Ideally, both the structural *and* the histological information should be obtained from the same frozen samples to prevent misinterpretation. In this paper we demonstrate a basic and inexpensive approach to obtain microtomographs of large bio-samples, e.g. frozen bones, which can be processed histologically afterwards.

METHODS: Fixation and freezing of the specimen were achieved by a self-made metallic perforated plate which was connected downside with a 20 cm long hollow copper tube and upside with 3 copper pins to fix the specimen (Fig. 1a). This device is then placed in a Dewar vessel filled with liquid nitrogen. The specimen is then freezed by the cold copper and the nitrogen which leaves the Dewar vessel through the holes in the plate. A second self-made cooling device is placed above the specimen. It consists of a stainless steel tank with a perforated floor. The tank is filled with dry ice. With this setup it is possible to keep the specimen frozen for at least 1 hour.

The samples were tomographically scanned with a maximum X-ray photon energy of E = 180 keV. Exploiting the X-ray beam divergence, the specimen was projected onto the detector plane with a maximum possible magnification of $m \approx 16.7$ given by the ratio of the focus-detector distance (1000 mm) to the focus-object distance (60 mm). The Dewar vessel was fixed to the turntable of the 7-axis manipulator and rotated about the rotary axis of that table. With the X-ray sensitive flat-panel detector, cone-beam projections of the specimen's region-of-interest were acquired at 1400 equally spaced angular positions of the turntable during circular CT-scanning. From these projections, tomograms (consisting roughly of 1800 × 1200 × 2000 voxels) were reconstructed. The achieved achieved voxel edge length was 12 µm (Fig. 1b).

After microtomographic imaging, the specimens were fixed in 4% formalin, dehydrated and embedded in Technovit 9100 New (Heraeus-Kulzer, Hanau, Germany). Using a microtome, sections (5 µm thick) were cut, placed onto poly-L-lysine-coated glass slides and specifically stained (for a detailed description see WILLBOLD and WITTE, 2010).

RESULTS, DISCUSSION & CONCLUSION: In this paper we demonstrate a useful basic setup for the microtomography of large frozen bio-samples. Thus, we are able to first make microtomographs of e.g. bone samples and then process these samples histologically (Fig. 2).

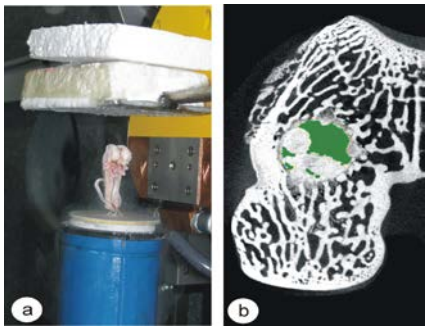

Fig. 1: *A rabbit condyle fixed in the cooling device (a) and a tomogram showing the bone structure and a degrading magnesium alloy (marked green)*

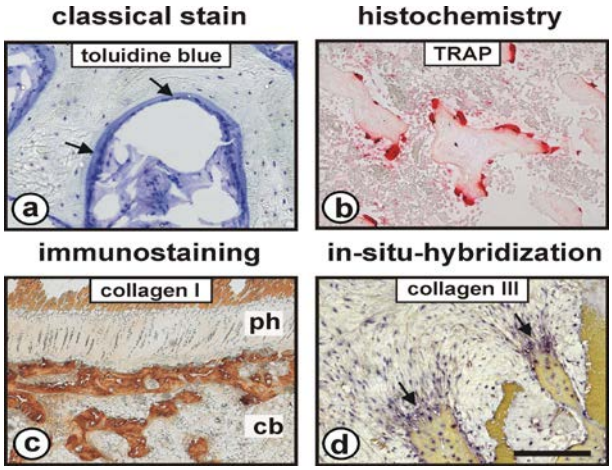

Fig. 2: Microphotographs of rabbit condyles stained with different histological staining methods. Scale bar = 200 µm.

REFERENCES: E. Willbold, F. Witte (2010) *Acta Biomater* **6**:4447 – 4455.

Optimization of the optical readout of PEEK cantilevers

Xue Zhao[1,2], Prabitha Urwyler[1], and Bert Müller[1]
[1]Biomaterials Science Center, University of Basel, CH. [2]Physics Department, ETH Zürich, CH.

INTRODUCTION: Using cantilever beam bending approach it is possible to determine the contractile forces of an ensemble of biological cells with nano-Newton resolution [1]. Si(100) wafers used as the cantilever material so far are rather expensive and difficult to handle because they are brittle. Owing to its biocompatibility 50 µm-thin polyetheretherketone (PEEK) is an interesting alternative to the silicon cantilevers.

Investigating the impact of substrate surface morphology on contractile cell forces we want to improve the surface of medical implants. Due to the limited reflectivity of PEEK, a reflecting layer such as a metallic film should be added. The aim of the study is the determination of the necessary gold thickness to obtain the required reflectance.

METHODS: A specially designed system was realized to measure the contractile cell forces of an ensemble of thousands cells. Light from a laser is reflected from the free end of the cantilever onto the position sensitive detector (PSD). As changes in cellular contraction or adhesion forces influence the curvature of the cantilever, the reflection angle and thus the final position of the laser beam on the PSD will change accordingly. This change in position is detectable allowing a quantification of the force using the Stoney formula [2]. We embossed the 50 µm-thick PEEK films on the rough side with plain pattern and 10 µm wide periodic pattern, using the hot embossing system HEX 03 (JENOPTIK Mikrotechnik GmbH, Jena, Germany). Through the thermal evaporator (BALZERS, Oerlikon, Switzerland) we coated the embossed PEEK films on the smooth side with a gold layer with thicknesses varying from 20 nm to 80 nm. First, we coated the polymer film with 4 nm chromium as sticky layer between PEEK substrate and gold film. The transmittance and reflectance of the embossed coated PEEK films are measured with the UV/VIS/NIR spectrometer Lambda 19 (Perkin Elmer, Massachusetts, USA).

RESULTS: The reflectance of the coated PEEK at the wavelength of 633 nm is of interest, because this is the wavelength of the laser used in the sensing system. As shown in Fig. 1, the reflectance increases with the gold coating thickness for both plain pressed and microstructured PEEK substrates according to the following relation:

$$R = 100\% - 55\% * \exp(-t/(28 \pm 2)\ \text{nm}).$$

The reflectance saturates for an infinite gold film and corresponds to 45%, if no gold film was deposited. The error bars of the reflectance and the gold thickness correspond to 2% and 2 nm, respectively.

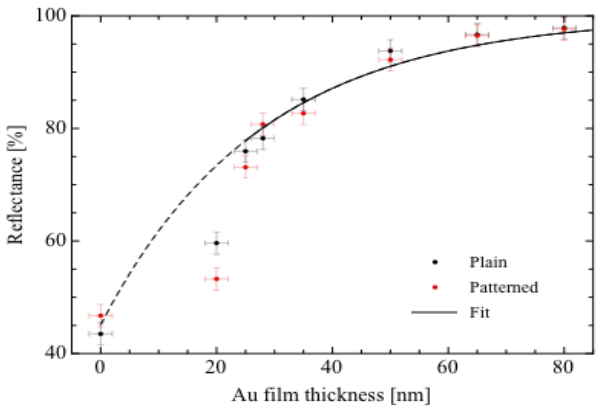

Fig. 1: Relation between reflectance and gold film thickness to determine an optimized film thickness for contractile cell force measurements.

DISCUSSION & CONCLUSIONS: There is no significant difference in reflectance between the plain and the patterned PEEK substrates. The curve progression only follows the added gold film thickness. Therefore, both data can be fitted simultaneously. The fit perfectly describes the data with one exception. For the 20 nm-thin gold film, the observed reflectance is well below the fitting curve. This behaviour can be explained by islanding, i.e. at 20 nm the gold film is not a confluent layer. Therefore, we conclude that a gold film with a thickness of 28 nm should be applied for experiments with PEEK substrates.

REFERENCES: [1]J. Köser, S. Gaiser, B. Müller (2011) *Eur Cells Mater* **21**:479-487. [2]G.G. Stoney (1909) Nature 172-175.

ACKNOWLEDGEMENTS: The hot embossing, gold coating and reflectance measurements were conducted at the Laboratory for Micro- and Nanotechnology (LMN) at the Paul Scherrer Institute (PSI). We thank the members of PSI-LMN for their support and assistance.

Bone cements for localized treatment of tumors through combined hyperthermia and chemotherapy

M Mohamed[1], V Bernau[2], H Hofmann[2], G Thalmann[3] G Borchard[1], O Jordan[2]

[1] *School of Pharmaceutical Sciences, University of Geneva, University of Lausanne, Geneva, CH.* [2]*Laboratory for Powder Technology, Ecole Polytechnique Fédérale de Lausanne (EPFL), Lausanne, CH.* [3] *Insel Hospital, Department of Urology, Bern, Switzerland*

INTRODUCTION: Bone metastases might be efficiently treated using intraosseous implants. In this view, we propose novel formulations that, once injected intraosseously, form a solid implant. Poly(methylmethacrylate) cements (PMMA) are relevant formulations already used in vertebroplasty. They can be loaded with both an anticancer agent (doxorubicin DOX) and superparamagnetic silica beads (SSB) for combining chemotherapy and hyperthermia, the latter being an effective adjuvant in cancer therapy.

METHODS: Cement was prepared by mixing poly(methylmethacrylate) and its monomer in presence of an initiator and an activator. SSB at 24% or 30% (w/w) and DOX at 2.5% (w/w) were loaded within the cement. Heating capacity was assessed by measuring cement temperature increase under an external alternating magnetic field (6 mT and 140 kHz). *In vitro* DOX release was carried out in a saline media at 37°C and the DOX was analyzed by spectrophotometry at 479 nm. *In vitro* toxicity of the implants was tested using XTT proliferation assay. Immortalized human prostate cancer cells, PC3, were incubated for 24h before the cell viability was measured and compared with a control of non-treated cell. Young modulus was determined by compression of Ø6x7 mm cylinders.

RESULTS: PMMA cement was able to generate heat in the range of 43-44 °C and displayed sustained release over at least 10 days. The release profiles were not influenced by the heat generated during a 25 min-hyperthermia session at 6 mT and 140 kHz, allowing further studies on the synergetic effects of hyperthermia and chemotherapy. The heating power of the implants, so-called specific power loss (SPL), indicates the potential for hyperthermia-induced antitumoral effect. Cement for intraosseous injection might provide some mechanical support to the weakened bone as the Young compression moduli are in the range of cancellous bone. *In vitro* toxicity of eluted DOX on PC3 cells shows preserved drug cytotoxicity.

Table 1. Characteristics of acrylic cements

	Cement	Cement-SSB 24% (w/w)	Cement-SSB 30% (w/w)
Elasticity [MPa]	186.1 ± 62.6	367.6 ± 130.6	239.1
SPL* [W/g]	-	1.97 ± 0.04	2.13 ± 0.06

***at 6mT**

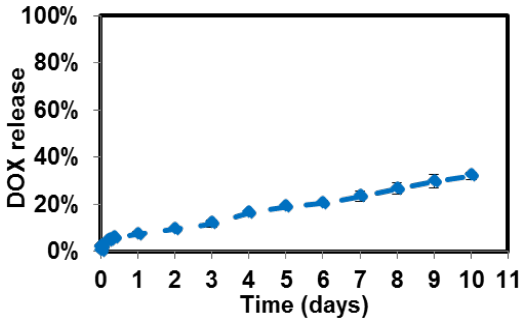

Fig. 1: DOX release profile of PMMA cement loaded with 24% SSB.

DISCUSSION & CONCLUSIONS: Acrylic cement was successfully loaded with doxorubicin and superparamagnetic nanoparticles, providing a sustained anticancer agent delivery and potential cytotoxic temperature. These data show within clinically acceptable parameters the feasibility of combining SPIONs for hyperthermia with local anticancer agent release.

ACKNOWLEDGEMENTS: Financial support was provided by the Swiss National Science Foundation (SNSF).